

Novel Naphthalene Diimides Synthesis, and Characterization as Probable Anticancer Agents

Saad Sami Awla Awla

Submitted to the
Institute of Graduate Studies and Research
in partial fulfillment of the requirements for the degree of

Master of Science
in
Chemistry

Eastern Mediterranean University
August 2021
Gazimağusa, North Cyprus

Approval of the Institute of Graduate Studies and Research

Prof. Dr. Ali Hakan Ulusoy
Director

I certify that this thesis satisfies all the requirements as a thesis for the degree of Master of Science in Chemistry.

Prof. Dr. İzzet Sakallı
Chair, Department of Chemistry

We certify that we have read this thesis and that in our opinion it is fully adequate in scope and quality as a thesis for the degree of Master of Science in Chemistry.

Assoc. Prof. Dr. Kerem Teralı
Co-Supervisor

Prof. Dr. Huriye İcil
Supervisor

Examining Committee

1. Prof. Dr. Huriye İcil

2. Assoc. Prof. Dr. Nur P. Aydınlık

3. Assoc. Prof. Dr. Kerem Teralı

4. Asst. Prof. Dr. Süleyman Aşır

5. Asst. Prof. Dr. Devrim Özdal

ABSTRACT

Naphthalene diimides (NDIs) have outstanding conjugation and photophysical properties which offer marvelous applications in various facets of industry from medicine to electronics. In medicine, NDIs can be used to interact with the guanine quadruplex and inhibit the proliferation of cancer cells by impairing the function of the telomerase enzyme that is responsible for replenishing the base units at the end of telomeres. Moreover, they can inhibit the function of acetylcholinesterase in Alzheimer disease. In addition, because of π -acidic property of NDIs, they can be used as transmembrane anion transporters between lipid layers.

In the present research, two symmetrical naphthalene diimides, 3 and 5, have been synthesized from the commercially available naphthalene dianhydride (NDA) with the primary amine in the presence of high boiling solvent. For compound 3, phosphate moiety was added to the imide positions in order to enhance the solubility in polar solvents. In the same way, for compound 5, adenine substituent was for being soluble in polar solvents and also was for having a strong interaction with the guanine quadruplex through π - π stacking, hydrogen bonding and other interactions. Optical properties for 3 and 5 in different solvents were measured. Compound 5 showed high molar absorptivity coefficient in the polar aprotic solvents such as DMAc, DMF and NMP. In addition to absorptivity coefficient, half width, oscillator strength and singlet energy were also being calculated.

FT-IR was performed in order to confirm the structures. Accordingly, a great consistency can be seen between the spectrum and the compounds.

Finally, we propose that the compounds might be used as anticancer agents and due to their planarity and rigidity of the molecules can also interact with the guanine quadruplex to prevent the telomerase to add base units and cause to cell division and proliferation.

Keywords: naphthalene diimide, anticancer, guanine quadruplex, characterization of NDI.

ÖZ

Naftalin diimidler (NDI'ler), tıptan elektroniğe endüstrinin çeşitli alanlarında harika uygulama alanı sunan olağanüstü bir konjugasyon ve fotofiziksel özelliğe sahip bileşiklerdir. Tıpta, guanin dörtlüsü ile etkileşime girmek ve telomerin sonuna kadar baz birimlerini yenilemekten sorumlu olan telomeraz enziminin işlevini engelleyerek kanser hücrelerinin çoğalmasını engellemek için kullanılabilirler. NDI'ler ayrıca Alzheimer hastalığında asetilkolinesterazın işlevini de inhibe edebilir. NDI'lerin π -asidik özelliğinden dolayı lipid tabakaları arasında transmembrane anyon taşıyıcısı olarak kullanılabilirler.

Bu araştırmada, iki simetrik naftalin diimid bileşiği 3 ve 5, ticari olarak temin edilebilen naftalin dianhidritten (NDA) birincil aminlerle yüksek kaynama noktasına sahip bir çözücü varlığında sentezlenmiştir. Polar solventlerde çözünürlüğü arttırmak için imid pozisyonlarına fosfat parçaları ilave edilerek 3 bileşiği elde edildi. Aynı şekilde, adenin süstitüentleri, polar çözücülerde çözünür olmaları ve ayrıca π - π etkileşimi, hidrojen bağı ve moleküller arası bağlar ile guanin dörtlü ile muhteşem bir etkileşime sahip olması için 5 bileşiğinin sentezinde kullanıldı. Farklı polaritede çözücüler kullanılarak 3 ve 5 için optik özellikler ölçüldü. Bileşik 5, DMAc, DMF ve NMP gibi polar aprotik çözücülerde yüksek molar absorpsiyon katsayısı göstermiştir. Soğurma katsayısına ek olarak, diğer fotofiziksel özellikler de hesaplanmıştır.

Sentezlenen maddelerin kimyasal yapılarını doğrulamak için FT-IR analizi yapıldı ve yapılan analize göre, spektrum ve bileşikler arasında büyük bir tutarlılık ortaya çıkmıştır.

Son olarak, tez kapsamında sentezlenen maddelerin birer antikanser ajanı olarak kullanılabileceğini ve moleküllerin düzlemselliği ve sertliği nedeniyle telomerazın baz birimleri eklemesini ve hücre bölünmesine ve çoğalmasına neden olmasını önlemek için guanin dörtlüsü ile etkileşime girebileceğini öneriyoruz.

Anahtar Kelimeler: naftalin diimid, antikanser, guanin dörtlüsü, NDI karakterizasyonu.

DEDICATION

To

My Family

ACKNOWLEDGMENT

First and foremost, I must thank my almighty who has given me everything. As he said “If you want to count up favors of me, it cannot be counted” I wish he will agree on me.

I am indebted to my mother, father, uncle Mohammed, uncle Salam, my aunts, my siblings, my cousins, friends and anyone who one day called me about my studying.

Special thanks should be sent to my dear supervisor Prof. Dr. Huriye İcil. She is not only my teacher but she has also acted as my mother and also my friend by giving me advices and considering about me. Similarly, I would like to thank Dear Assoc. Prof. Dr. Kerem Teralı for his co-supervision and information as well.

I would like to thank all organic group members in Eastern Mediterranean University. Dear Dr. DUYGU, Arwa, Selin, Pelin, Blerta and specifically, Dear Dr. Basma Basil and Meltem dinleyici for being with me in the lab and showing the procedure thanks again for everyone of you..

I should also send my gratitude for Rebwar Saeed, a PhD Student in Chemistry, and his wife, Mrs. Bzhar Sardar, the Kurdish family in Cyprus for being with me and helping me in many situations. I wish one day I could repay their debt.

During my master I have known people, but two of them are very special and they are dear Dr. Faisal Suleiyman and Dr. Amro Al Ammaren I wish them success.

TABLE OF CONTENTS

ABSTRACT	iii
ÖZ	v
DEDICATION	vii
ACKNOWLEDGMENT	viii
LIST OF TABLES	xi
LIST OF FIGURES	xii
LIST OF SYMBOLS AND ABBREVIATIONS	xv
1 INTRODUCTION.....	1
1.1 Naphthelene Diimide.....	1
1.2 Cancer.....	5
1.3 Cytotoxicity	7
2 THEORETICAL.....	9
2.1 Deoxyribonucleic Acid.....	9
2.1.1 DNA Intercalating Agent	10
2.2 The Interaction Between NDI and G–4.....	11
3 EXPERIMENTAL	17
3.1 Materials	17
3.1.1 Instruments.....	17
3.2 Method of Synthesis for 3 and 5	18
3.2.1 Synthesis of N,N'– bis [(2– (dihydrogenphosphoryl) ethyl)]–1,4,5,8– naphthalene diimide (3)	18
3.2.2 Synthesis of N,N'–bis(7H–purinyl)–1,4,5,8–naphthalene diimide (5).....	19
3.3 Mechanism of the Reaction	21

4 DATA AND CALCULATION.....	23
4.1 Calculation of Optical Parameters.....	23
4.1.1 Molar Absorption Coefficients (ϵ_{max}).....	23
4.1.2 Half Width of Selected Absorption $\lambda_{1/2}$	25
4.1.3 Theoretical Radiative Life Times (τ_0).....	27
4.1.4 Calculation of Fluorescence Rate Constant (K_f).....	28
4.1.5 Oscillator Strength (f).....	29
4.1.6 Singlet Energies (E_s).....	30
5 RESULTS AND DISCUSSION	53
5.1 Synthesis of N,N'-bis(2-(dihydrogenphosphoryl)ethyl)-1,4,5,8- naphthalene diimide (3) and IR spectra analysis	53
5.2 Synthesis of N,N'-bis(7H-purinyl)-1,4,5,8-naphthalene diimide (5) and IR Spectra Analysis	54
5.3 Solubility of the 3 and 5	54
5.4 Interpretation of UV / Vis absorption for 3 and 5	55
6 CONCLUSION	57
REFERENCES	59

LIST OF TABLES

Table 4.1: Concentration, maximum wavelength and absorbance for 5 in DMAc....	24
Table 4.2: Molar absorption coefficients of 5 in various solvents	25
Table 4.3: Half width of 3 and 5 in various solvents	27
Table 4.4: Theoretical radiative life time (ns) of 5	28
Table 4.5: Theoretical fluorescence rate constant for 5 in various solvents	29
Table 4.6: Oscillator strength of 5 in various solvents.....	29
Table 4.7: Singlet energies of 5 in various solvents	30
Table 4.8: Singlet energies of 3 in various solvents	31
Table 4.9: Photophysical properties of 3 and 5 in various solvents.....	32
Table 5.1: Solubility test of 1, 3 and 5	55

LIST OF FIGURES

Figure 1.1: General structure of the NDI	2
Figure 1.2: Structure of N,N' –bis[(2 – (di hydrogenphosphoryl) ethyl)] – 1,4,5,8 – naphthalene diimide (3).....	4
Figure 1.3: Structure of N,N'-bis(7H-purinyl)-1,4,5,8-naphthalene diimide (5)	4
Figure 1.4: The hallmarks of cancer (Hanahan & Weinberg, 2011).....	7
Figure 1.5: Reduction of MTT for the formazan	8
Figure 2.1: Amino acids in DNA and RNA.....	10
Figure 2.2: Binding process between bases of the DNA with the intercalator agent binding	11
Figure 2.3: Structure of the G–4 with the metal	13
Figure 2.4: Possible G–4 intramolecular structure	14
Figure 3.1: Synthesis of N,N'– bis[(2– (dihydrogenphosphoryl)ethyl)]– 1,4,5,8 – naphthalene diimide (3) from (2) and (1).....	19
Figure 3.2: Synthesis of N,N'–bis(7H–purinyl)–1,4,5,8–naphthalene diimide (5) from (1) and (4)	20
Figure 4.1: Absorbance Vs. concentration of 5 in DMAc	24
Figure 4.2: Estimation of half width for 3 in NMP.....	26
Figure 4.3: FT–IR spectrum of 1,4,5,8– Naphthalenetetracarboxylic dianhydride....	33
Figure 4.4: FT–IR spectrum of 2–aminoethyl dihydrogen phosphate, amine (2)	34
Figure 4.5: FT–IR spectrum of 7H–purine–6–amine, amine (4)	35
Figure 4.6: FT–IR spectrum of N,N'– bis[(2–(dihydrogenphosphoryl)ethyl)]– 1,4,5,8 –naphthalene diimide	36

Figure 4.7: FT-IR spectrum of 1 and 3.....	37
Figure 4.8: FT-IR spectrum of N,N'-bis(7H-purinyl)-1,4,5,8-naphthalene diimide	38
Figure 4.9: FT-IR spectrum of 1 with 5	39
Figure 4.10: UV / Vis spectrum of N,N'- bis[(2-(dihydrogenphosphoryl) ethyl)]- 1,4,5,8- naphthalene diimide in DMAc.....	40
Figure 4.11: UV / Vis spectrum of N,N'- bis[(2-(dihydrogenphosphoryl) ethyl)]- 1,4,5,8- naphthalene diimide in DMF	41
Figure 4.12: UV / Vis spectrum of N,N'- bis[(2-(dihydrogenphosphoryl)ethyl)]- 1,4,5,8-naphthalene diimide in DMSO	42
Figure 4.13: UV / Vis spectrum of N,N'- bis[(2-(dihydrogenphosphoryl)ethyl)]- 1,4,5,8- naphthalene diimide in NMP	43
Figure 4.14: UV / Vis spectrum of N,N'- bis[(2-(dihydrogenphosphoryl)ethyl)]- 1,4,5,8- naphthalene diimide in TFAc.....	44
Figure 4.15: UV / Vis spectrum of N,N'- bis[(2-(dihydrogenphosphoryl)ethyl)]- 1,4,5,8-naphthalene diimide in various solvents	45
Figure 4.16: UV / Vis spectrum of N,N'-bis(7H-purinyl)-1,4,5,8-naphthalene diimide in CHL	46
Figure 4.17: UV / Vis spectrum of N,N'-bis(7H-purinyl)-1,4,5,8-naphthalene diimide in DMAc	47
Figure 4.18: UV / Vis spectrum of N,N'-bis(7H-purinyl)-1,4,5,8-naphthalene diimide in DMF	48
Figure 4.19: UV / Vis spectrum of N,N'-bis(7H-purinyl)-1,4,5,8-naphthalene diimide in DMSO.....	49

Figure 4.20: UV / Vis spectrum of N,N'-bis(7H-purinyl)-1,4,5,8-naphthalene diimide in NMP	50
Figure 4.21: UV / Vis spectrum of N,N'-bis(7H-purinyl)-1,4,5,8-naphthalene diimide in TFAc	51
Figure 4.22: UV / Vis spectrum of N,N'-bis(7H-purinyl)-1,4,5,8-naphthalene diimide in various solvents	52

LIST OF SYMBOLS AND ABBREVIATIONS

A	Adenine
Å	Armstrong
CHL	Chloroform
cm	Centimeter
°C	Celsius
C	Concentration
C	Cytosine
DMAc	Dimethyl Acetamide
DCM	Dichloromethane
DMF	Dimethylformamide
DMSO	Dimethyl Sulfoxide
DNA	Deoxyribonucleic Acid
Es	Singlet Energy
ϵ_{max}	Maximum Extinction Coefficient / Molar Absorptivity
F	Oscillator Strength
FT-IR	Fourier Transform Infrared Spectroscopy
G-4	Guanine Quadruplex
G	Guanine
HIV	Human Immunodeficiency Virus
KBr	Potassium Bromide
K_d	Rate Constant of Radiationless Deactivation
K_f	Fluorescence Rate Constant
MTT	(3-(4,5-dimethylthiazole-2-yl)-2,5-diphenyltetrazolium bromide

Nm	Nanometer
NMP	N-methylpyrrolidinone
NDA	1, 4, 5, 8-Naphthalenetetracarboxylic Dianhydride
NDI	Naphthalene Diimide
RNA	Ribonucleic Acid
T	Thymine
TFA	TrifluoroAcetic Acid
TLC	Thin Layer Chromatography
τ_0	Theoretical Radiative Lifetime
UV	Ultraviolet
UV / Vis	Ultraviolet Visible Light Absorption
λ	Wavelength

Chapter 1

INTRODUCTION

1.1 Naphthalene Diimide

Naphthalene diimides (NDIs) are polycyclic non-aliphatic compounds with electron-carrying characteristics. They are a smaller member for the rylene diimide which both of them have an excellent electrochemical and photochemical properties integrate with the thermal stability. The most prominent compounds in the rylene diimide family are both naphthalene diimide and perylene diimid, which have excellent role in various facets of industry (Zhan et al., 2011). Both naphthalene diimide and perylene diimide are out-standing materials for the π -conjugation as a member in the heteroatom molecules (Aleshinloye et al., 2015).

In the beginning of the 1930s, the study of the naphthalene diimide was initiated by Vollmann et al. Being a compact, not electron rich and ability for self-assembly are the core features of the NDI (Bhosale et al., 2008).

Naphthalene diimides are robust and planar organic compounds with high melting point (Guha et al., 2012). Due to its facility of preparation, redox property, electromagnetic radiation absorption, tendency for electron, and lowest unoccupied molecular orbital position make naphthalene diimide a fabulous nominee for the n-type semiconductor compounds (Al Kobaisi et al., 2016). Being stable in the thermodynamically facet can be attained because of the self-assembly

of the naphthalene diimide which are linked together via non-covalent interaction (Whitesides et al., 1995). Naphthalene diimide is considered as a π -acid molecule because of their ability to receive electrons and then it can interact with the anions, which refers to π -anion interaction (Guha & Saha, 2010).



Figure 1.1: General structure of the NDI

Naphthalene diimide has four polar groups on the shoulder with lipophilic group at the core and is usually soluble in low polarity solvents such as chloroform (CHL), toluene, dichloromethane (DCM) and also in the polar aprotic solvents like dimethyl sulfoxide (DMSO), dimethylformamide (DMF), acetonitrile. Solubility of the naphthalene diimide generally relies on the moieties on the imide groups with long and bulky non-aromatic substituents promote the solubility (Bhosale et al., 2008).

Naphthalene diimide can be used in various areas from electronics to biomedicine (Guha et al., 2012). In many electrical fields, naphthalene diimide can be used. For instance, as a conducting material, optical brightening, electrophotography, photosynthesis reactions and in the laser dyes as well. Owing to π - π stacking, electron

donor and acceptor and self-organization naphthalene diimide derivatives are used in the organic electronics. Since it is an n-type semiconductor, it is popularly used in the area of organic field-effect transistors (Ozser et al., 2003). Because of their redox and optical features NDIs can be used in the nanotechnology, physics, and material chemistry (Ghule et al., 2015).

In medical chemistry, naphthalene diimide derivatives can be used to reduce the activity of enzymes. For example, they can prevent the action of the acetylcholinesterase (Tumiatti et al., 2008). In addition, to deliver anions beyond lipid bilayer membrane, electron-deficient or π -acidic aromatic molecule is required for π -anion interaction and then the anion could through over the slide (Marenda & Matile, 2009). Furthermore, elongate core-naphthalene diimide has displayed a promotion for guanine quadruplex selectivity and binding, which serves as an anti-human immunodeficiency viruses (HIV) agent (Tassinari et al., 2018). More crucially, ability of naphthalene diimide to bind with guanine quadruplex has been considered as a decent ligand (Doria et al., 2019)

Properties of NDI can be altered significantly by adding different moieties at various positions. From the imide position functional groups can be added. Likewise, from the core position, which each of them manages the properties of the compound differently (Yue et al., 2010).

Core naphthalene diimides are the places where the carbon number is 2, 3, 6, and 7. Core-naphthalene diimide is responsible for the photophysical properties, electronic properties, various colors and conductivity of the compound (Bhosale & Bhargava,

2012). Core-naphthalene diimide chromophore effects the redox and spectral properties of the compound (Polander et al., 2012)

Although imide positions have little impact on the optical and electronical properties, it is responsible for the aggregation and solubility of the compound (Polander et al., 2012). Because of the node existence in the imide atom it leads to completely separate naphthalene diimide from inductive and mesomeric effect and imide positions do not affect the electronic properties (Sommer, 2014).

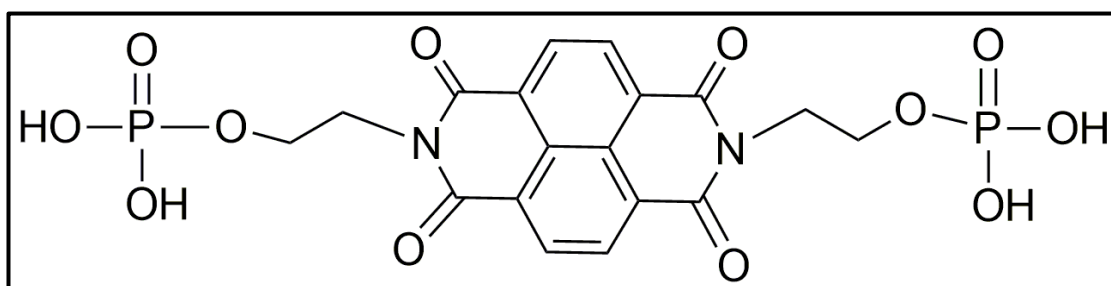


Figure 1.2: Structure of N,N'-bis[(2-(dihydrogenphosphoryl)ethyl)]-1,4,5,8-naphthalene diimide (3)

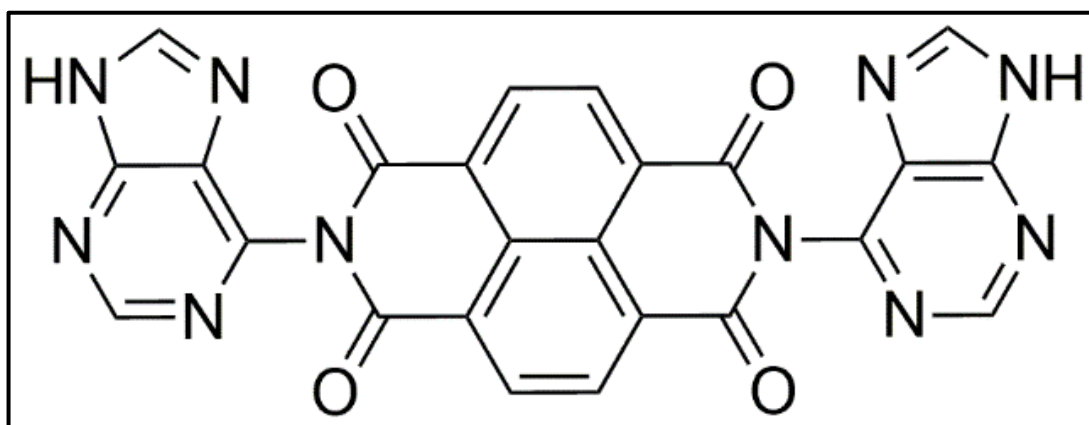


Figure 1.3: Structure of N,N'-bis(7H-purinyl)-1,4,5,8-naphthalene diimide (5)

1.2 Cancer

Cancer can be defined as one of the diseases which is caused by an increase in the number of cells with no control as a result of malfunction of signaling pathways, which are under control in normal cases. Cancer can spread quickly and invade other tissues (McCauley et al., 2013). Cancer is considered as an illness of the cells (Doll & Peto, 1981). In the 21st century, it is believed that cancer becomes a main cause of death and one of the most important barriers to rise life expectancy around the globe. The reasons, which cause cancer, are ambiguous but it is believed that ageing, growing of the population and socioeconomic factors are fundamental causes. According to the GLOBOCAN survey in 2018 for 185 countries, there were above 18 million new cases for cancer integrate with above 9 million cases for cancer death. Among various types of cancer for both genders, lung cancer was identified as most frequently with 11.6% and 18.4% for new cases and death in turn. Moreover, prostate cancer was the second most fatal one for men. On the other hand, breast cancer was the most dangerous one for women (Bray et al., 2018).

Cancer is classified as a chronic illness. In order to combat this disease, World Health Organization (WHO) has proposed ideas about cancer prevention. Firstly, by early diagnosing of the oncogene, which prevents 33%. The second one is by proper treatment mechanism in order to soar the ratio of the survival of the infected patient by 33%. Cancer is intertwined with the inflammation. In other words, inflammation induces tumor properties and then satisfy almost all hallmarks of cancer and finally toward a malignant tumor (Cao et al., 2011).

In normal situation, non–cancer cells are told to be divided or proliferated whenever it is required. That is, they only function whenever necessary and being arranged and controlled completely. Cancer cells, on the other hand, divide without being told to do that, chase their desire, and conquer other tissues (Weinberg, 1996).

Mutation of genes plays a pivotal role in the cancer. It would be fair enough if doctors call cancer a “genetic illness” (Hausman, 2019). Impairment of various segments of biological system is considered to pose a cancer (Hornberg et al., 2006). Hallmarks of the cancer illustrates the common properties of all types of cancer in more detailed way with explicitly as explained in Figure 1.4 (Hanahan & Weinberg, 2011).

In addition, one perilous point which is evaluated that about eighty percent of the cancer causes are because of environmental and sedentary lifestyle, which can be stopped (Doll & Peto, 1981).

Cancer can be divided into two groups: benign and malignant. The difference between them is well–known. The latter one is more fatal and has the ability to metastasis and invade other tissues with swift growth (Van Raamsdonk et al., 2009).

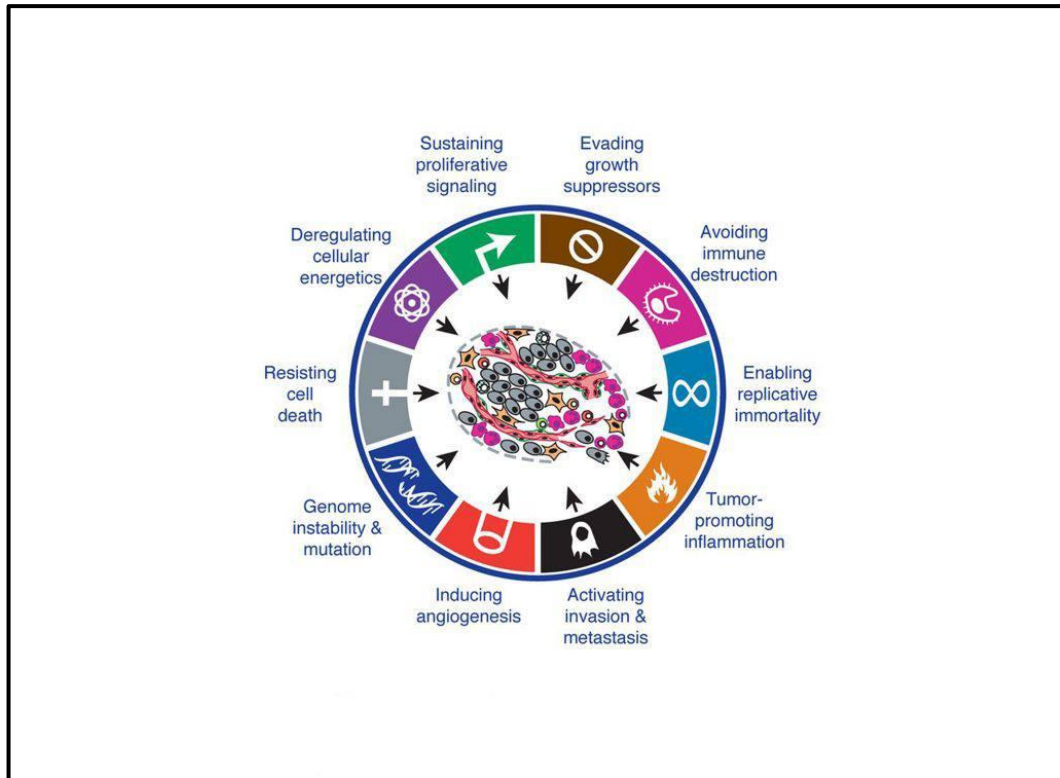


Figure 1.4: The hallmarks of cancer (Hanahan & Weinberg, 2011)

Metastasis is said to be the major cause of cancer death. Either losing or mutation occurred at p53 will lead to make a suitable environment for metastasis (Gao et al., 2020).

1.3 Cytotoxicity

One of patterns to extend patient's life is by using chemotherapy. Activity and proliferation of the cells can be checked by the (3-(4,5-dimethylthiazole-2-yl)-2,5-diphenyltetrazolium bromide (MTT assay), which is considered to be a sensitive and dependable method. Upon adding the agent and reagent to the cancer cells, two types of reaction are expected. If the cells die after applying the agent, they do not show any reaction and the color of the MTT remains as light yellow. If the cells are still alive, however, the color of reagent changes to the purple color by the action of the mitochondria reductase inside the mitochondria and an insoluble formazan will be produced (Senthilraja et al., 2015).

Before adding the agents, plates put inside the incubator for about 4–5 days at 37 °C in order to undergo several cell divisions and growth. About the alive cells, both plasma and mitochondria membrane are crossed by the MTT and it is reduced by the NADPH. Forming an insoluble product is one of the flaws of the MTT assay.

Solubility is crucial in this method UV / Visible is used in this method. Being a water soluble is outstanding because it does not cause any harm for the protein agents such as antibodies. Most of the compounds, unfortunately, soluble in the organic solvents. DMSO and DMF are the most common ones. For the cancer cells in the cell culture, DMSO is more preferable because it is believed to be less toxic for them. According to many experiments, agents usually work under micromolar levels but stock solution should be prepared from millimolar and then create a serial dilution in order to decline the toxicity of the organic solvents (Burton., 2005).

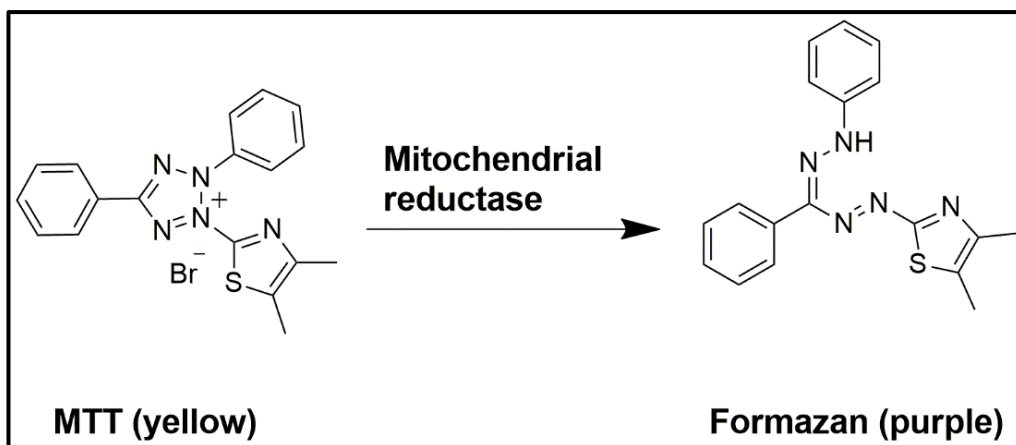


Figure 1.5: Reduction of MTT for the formazan

Chapter 2

THEORETICAL

2.1 Deoxyribonucleic Acid

Watson and Crick discovered the helical structure of the deoxyribonucleic acid (DNA) in 1953 with now well-known features. Because DNA manages the functions of the cell it is believed to be one of the out-standing sources of treatment for genetic disorder, such as cancer. After Lerman had found out the interaction between DNA with acridine, he suggested the effect of anticancer compounds with DNA via intercalation (Martinez & Chacon–Garcia, 2005).

Two polynucleotide chains are intertwined with each other to form DNA strand. A nitrogen-containing ring, 5-carbon sugar and the phosphate are the composition of each nucleotide. Nucleotides are adenine (A), Guanine (G), cytosine (C) and thymine (T). Formation a bond between sugar and the phosphate is led to form a backbone of the DNA (Alberts et al.,2002).

The double helix structure of DNA illustrates how complementary bases interact with each other via hydrogen bond in opposite strands either cytosine with guanine or adenine with thymine. All of the genetic information is carried by the DNA which is the essential living part of the organisms. The act of those nucleotides are vital for creating and recognizing each other in opposite strands for DNA replication and duplication (Seeman, 2003).

Telomere (cap of the DNA) has several crucial duties which are involving in the senescence, replication, and protection of the chromosome (Sun et al., 1997). Remaining of telomere is vital to transform the oncogene cells and operate telomere maintenance process is crucial to become an immortal cell (Doria et al., 2012). As long as DNA replicates, telomere length gets shorter and possess constraint of proliferation and cell growth (Asamitsu, Obata, et al., 2019). One of the enzymes which has been considered as anti-cancer drugs is telomerase, which can be found in tumors and as one of the parameters for identifying the cancer (Sato et al., 2005). It is believed to be overexpressed in more than ninety percentage of cancer cells and the opportunity to still alive in ill person is more with lower telomerase expression compare with higher telomerase expression (Asamitsu, Obata, et al., 2019).

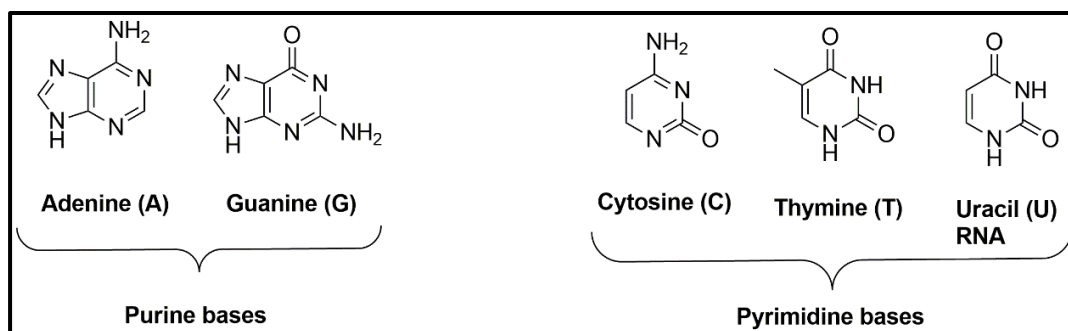


Figure 2.1: Amino acids in DNA and RNA

2.1.1 DNA Intercalating Agent

In cancer therapeutics, DNA structure has been chosen as a target. DNA target drugs also can perform as an enzyme inhibitor. For instance, inhibition of the topoisomerase, which is responsible for unwinding DNA strands (Hurley, 2002).

Intercalators are compounds with having a planar structure, polycyclic, heteroatomic compounds with nearly the same size of the base pairs of the DNA. They do not

interact with the DNA covalently but instead via H-bond, electron transfer and van der Waals force while enter into the DNA perpendicularly (Tumiatti et al., 2009). Furthermore, in order to attain DNA affinity, amine groups should be added so that interact with the DNA via the hydrophobic and electrostatic interaction. More vitally, naphthalene imide and naphthalene bis-imide have displayed strong DNA intercalator because of it is structure and fulfilment of the conditions (Tandon et al., 2017).

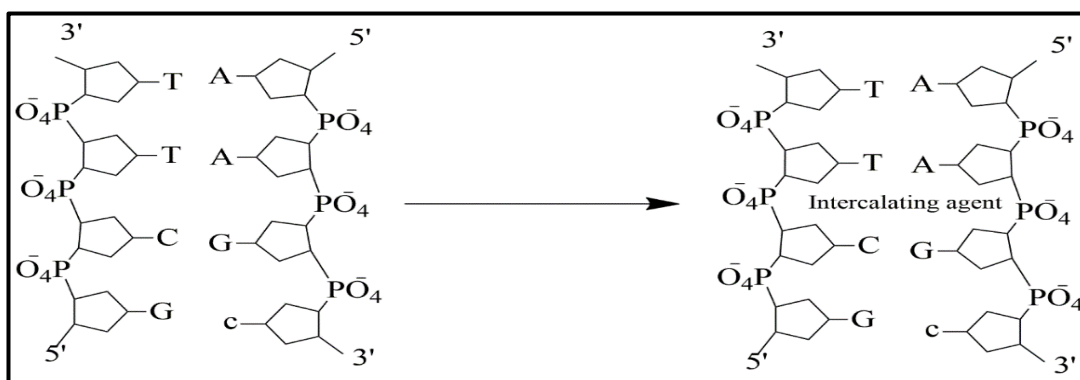


Figure 2.2: Binding process between bases of the DNA with the intercalator agent binding

2.2 The Interaction Between NDI and G-4

Guanine quadruplex has a square planar structure of four Guanine nucleotide base attached to each other via Hoogsten H-bond (Nadai et al., 2018). G-4 has three-dimensional, four-stranded shape with nucleotide base loaded of the Guanine. TTAGGG sequence can be seen on the end of the telomere in the single stranded DNA, which then have the ability to form larger well-arranged structure known as G-4 (Prato et al., 2015). In tumor cells, preserve this G-4 structure has proved to halt the activity of the telomerase (Doria et al., 2016).

The quadruplex can be found in both telomeric end of the chromosome as well as in the oncogene promoter such as *c-KIT*, *c-MYC*, and *BCL2*. For the latest one, G-4

binding molecules can quell the transcription and translation (Sato et al., 2018). Moreover, G–4 is also doable to be formed in ribonucleic acid because of its pliability, sensitivity for alterations, and single stranded state (Asamitsu, Bando, et al., 2019).

Proto–oncogenes are a sign to influence cell division. After mutation, possess to overexpression of the proteins and lead to cell proliferation (Weinberg, 1996). c–MYC in proliferation has a role as a transcriptional activator. In oncogene cells, c–MYC is said to be active compound. Although it is believed to halt the activity of it is a suitable cancer therapy, because of their not long half–time, an immense dimension, and unstructured nature it could not attain great attentions (Asamitsu, Obata, et al., 2019). In addition, MYC proteins influence genes which lead cell growth. Overexpression of MYC can be seen in majority of cancer cells (Weinberg, 1996).

Releasing Bcl–2 in more than normal ratio is known to halt apoptosis, lead to metastasis in some oncogene types and it also has a role in drug resistance. Decline the overexpression of Bcl–2 can lead to soar the effectiveness in cancer drugs and it is role as a target in therapeutic drug has been proved (Gunaratnam et al., 2018).

Bioinformatic evidence has displayed that more than 360000 DNA sequences have the ability to form G–4 (Ang et al., 2016). In normal cells, about 43% of genes have the G–4 in their promoter. Impressively, nearly three quarter of genes in cancer cells have the probability having the G–4. Like other nucleic acids, G–4 is considered to be highly negative species and if there is a cation molecule, a strong interaction can be achieved. Despite binding between ligands and G–4, they also have the affinity to bind with the secondary structure of the DNA (Huppert, 2008).

Forming G–4 from the single strand DNA by binding hinders the activity of several enzymes (Zahler et al., 1991). For example, telomere in the DNA is replenished by the telomerase enzyme, which is active in about 85% of cancer cells and it also incites the cell division and proliferates of cancer cells (Mancini et al., 2016). Even though this enzyme is crucial for the immortality of cancer cells, it is not active in majority of normal cells (Takeuchi et al., 2019).

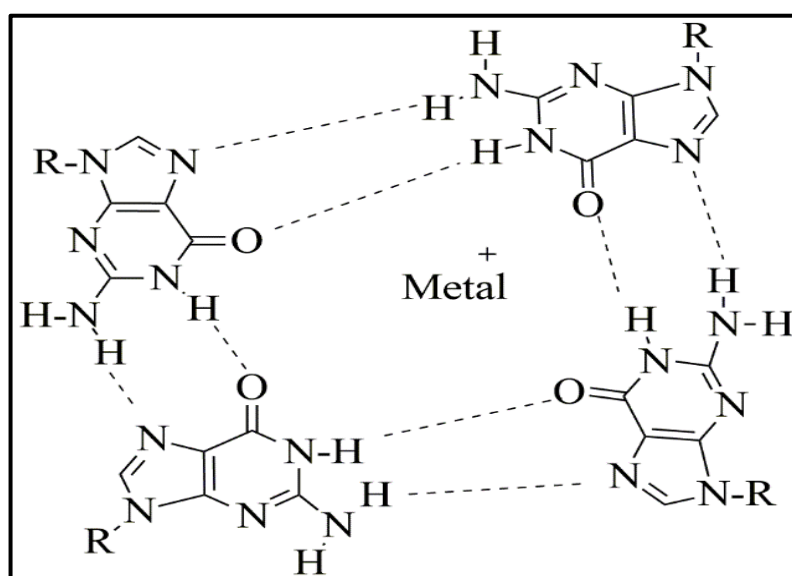


Figure 2.3: Structure of the G–4 with the metal

Various structure for the G–4 is doable, all of them might be parallel, one antiparallel and the others are parallel, or one pair is in opposite with other pair and vice versa. The main reason to have variety of the structure is related to the glycoside bond between sugar and the guanine. The shape becomes G–4 symmetry if the strands are parallel and anti-conformation formation can be seen for the bases and same size of the grooves between backbones are also required. Antiparallel, on the other hand, syn structure is necessary for the bases which affects the orientation of the backbone and grooves will be in an unlike size. The structure of the strands can be fused with each

other via the loops (Huppert, 2008). Their different structure is explained in Figure 2.4 (Asamitsu, Obata, et al., 2019).

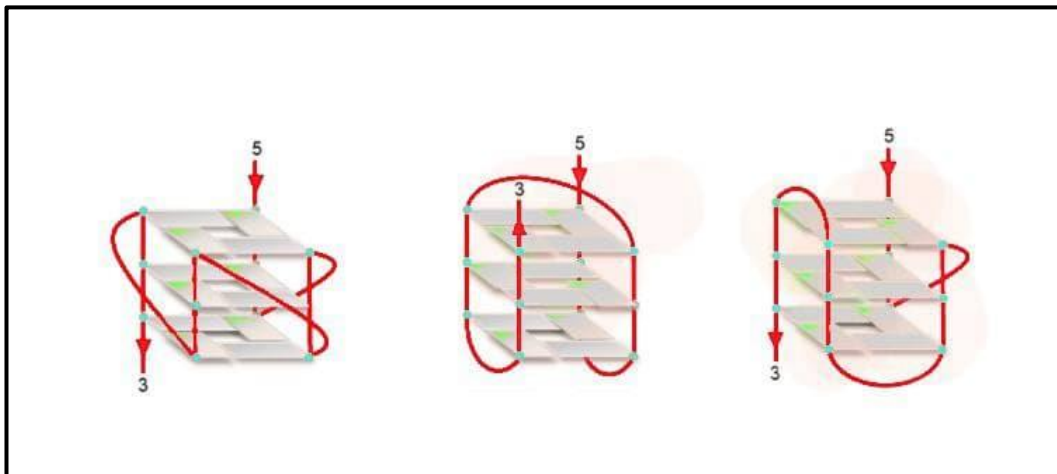


Figure 2.4: Possible G-4 intramolecular structure

Water solubility of NDI is in our concern since their water solubility is vital for biological aspects. In both imide and C-NDI, water soluble substituents can be added. Both anionic and cationic moieties can be added to enhance water solubility. Likewise, non-ionic groups can trigger water solubility by having several polar groups because those groups can reduce π - π aggregation via of steric hindrance or electrostatic repulsion forces (Sun et al., 2016).

Selecting of the out-standing ligand to interact with G-4 is not a random process, but it has some policies. For example, if the ligand has a planar structure rather than twisted one, it would be excellent because they interact with the G-4 through π - π stacking. In addition, intramolecular and intermolecular of the G-4 should be considered. That is, some ligands prefer to bind to parallel or hybrid, whereas others would like to interact with anti-parallel and vice versa (Asamitsu, Bando, et al., 2019). Furthermore, polycyclic compounds with substitution at various places (Vasimalla et al., 2017).

What is more, positive and protonable functional groups is one of the most strategies to be a good ligand (Doria et al., 2012). By elongating the planar surface of the NDI, the desire for G–4 binding would rise. In addition, the biological action and DNA affinity would considerably decline by detaching of the cationic moieties (Micco et al., 2012). What is more, little selectivity displayed for G–4 via disubstituted NDI, tri and tetra substituted NDI, however, demonstrated large affinity toward it (Nadai et al., 2011).

G–4 ligands have displayed low selectivity toward G–4 since in the genome same G–4 skeleton can be noticed between various G–4 forms (Asamitsu, Obata, et al., 2019). Because of the planarity of structure, which affects the binding with G–4, ability to form π – π interaction, easily preparation, and versatility of the NDIs, they have been attractive compounds for binding with the G–4. Via C–NDI both G–4 and NDI interact with each other through π – π interaction. Moreover, since it contains H₂O they interact via hydrogen bonding. In addition, if cationic moiety is available on the NDI, it would interact by electrostatic interaction with the negative phosphate (Prato et al., 2015). The effect of NDIs on G–4 have seen by telomere uncapping which results DNA devastating and the process of senescence. Moreover, the oncogenic transcription and translation are hindered. In addition, DNA insecure via DNA end fusion, which leads to the programmed cell death. This cell cycle relies on several parameters. For instance, it is different in various cells, the character of the ligand, NDI, and binding and selectiveness for a specific G-4 (Hampel et al., 2013). Research have displayed that cyclic NDIs have larger affinity toward G–4 rather than double stranded DNA. In addition, it is also believed that imide position is more responsible for decreasing the affinity toward double stranded DNA (Esaki et al., 2014). Since the imide position is

generally responsible for the G–4 stabilization, in this facet, the carbon number of 2–3 with uneven length have proved to be a marvelous G–4 stabilizer and promote cell proliferation (Al Kobaisi et al., 2016).

Chapter 3

EXPERIMENTAL

3.1 Materials

1,4,5,8-Naphthalenetetracarboxylic dianhydride (1), isoquinoline, 2-aminoethyl dihydrogen phosphate (2), 7H-purine-6-amine (4), and zinc acetic anhydride were attained from Sigma-Aldrich without further purification. Similarly, solvents such as methanol, ethanol, acetone, chloroform were also obtained from Sigma-Aldrich. m-cresol and isoquinoline stored over 4 Å molecular sieves. Molecular sieves of size 4Å (4–8 mesh) which supplied by Sigma-Aldrich were activated at 500 °C and used for drying liquid reagents. About spectroscopic analysis, pure spectroscopic grade solvents were used without further purification.

All the reactions were controlled by thin layer chromatography (TLC aluminium sheets 5*10 cm silica gel 60 F₂₅₄) which visualize by UV light and/or placing the plate in acidic vanillin.

3.1.1 Instruments

Infrared spectra were recorded with potassium bromide pellets using JASCO FT/IR-6200 (fourier transform infrared spectrometer).

Ultraviolet Absorption spectra (UV) was measured with Cary-100 UV-Visible Spectrophotometer.

3.2 Method of Synthesis for 3 and 5

The aim of this thesis is to synthesize two novel (NDI)s for biological applications. In the below section, the synthesis of 3 and 5 from commercially available NDA are explained respectively.

3.2.1 Synthesis of N,N'-bis [(2-(dihydrogenphosphoryl)ethyl)]-1,4,5,8-naphthalene diimide (3)

The suspension of (1) (1.002 g, 3.73×10^{-3} mol), (2) (2.12 g, 0.015 mol) and zinc acetate (0.818 g, 3.73×10^{-3} mol) in 40 mL of isoquinoline was stirred under inert nitrogen atmosphere at room temperature, the mixture was more stirred at 80 °C for 8 h, 100 °C for 6 h, 120 °C for 7 h, 160 °C for 4 h and 200 °C for 9 h. 250 mL of acetone was refrigerated for 30 min and then the reaction mixture was poured into it, refrigerated for 1 day for complete precipitation. The resulting precipitate was filtered and dried at 100 °C under vacuum filtration, and the crude product was purified by acetone soxhlet to get rid of high boiling solvent, zinc acetate and impurities.

Yield; 85.5 % (1.92 g); **Color;** Black; **Melting point** > 300°C

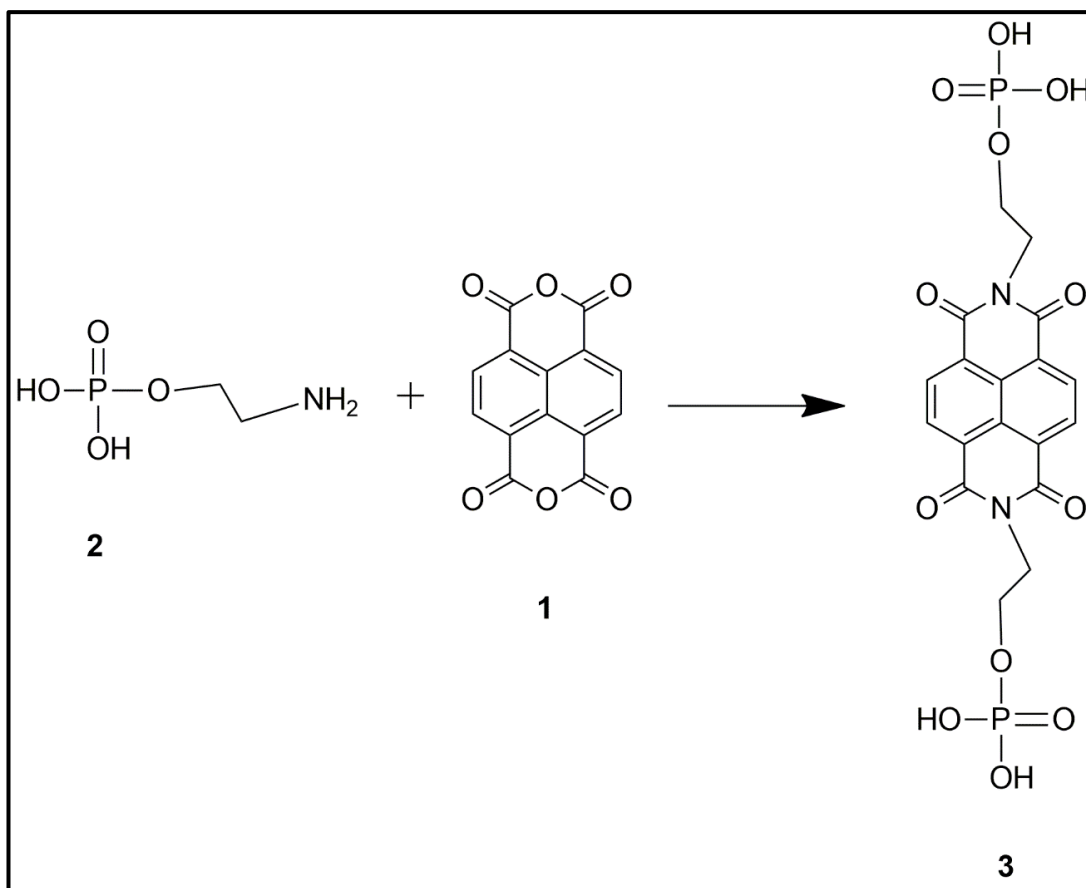


Figure 3.1: Synthesis of N,N'-bis[(2-(dihydrogenphosphoryl)ethyl)]-1,4,5,8-naphthalene diimide (3) from (2) and (1)

3.2.2 Synthesis of N,N'-bis(7H-purinyl)-1,4,5,8-naphthalene diimide (5)

About (4) with (1), same quantity of (1) was used (1.002 g, 3.73×10^{-3} mol), (4) (2.57 g, 0.015 mol) and zinc acetate (0.818 g, 3.73×10^{-3} mol) in 40 mL of isoquinoline was reacted under inert nitrogen atmosphere at room temperature, the reaction was further carried out at 80 °C for 8 h, at 100 °C for 5 h, at 120 °C for 7 h, at 160 °C for 4 h and 200 °C for 9 h. 250 mL of ethanol was refrigerated for 30 min and then the reaction mixture was poured in it, refrigerated for 1 day for complete precipitation and then filtered by vacuum filtration and dried at 100 °C under vacuum oven and then the crude product put in the chloroform soxhlet to get rid of the extra amine and impurities.

Yield; 65.2 % (1.87 g); **Color;** Greenish brown; **Melting point** > 300 °C

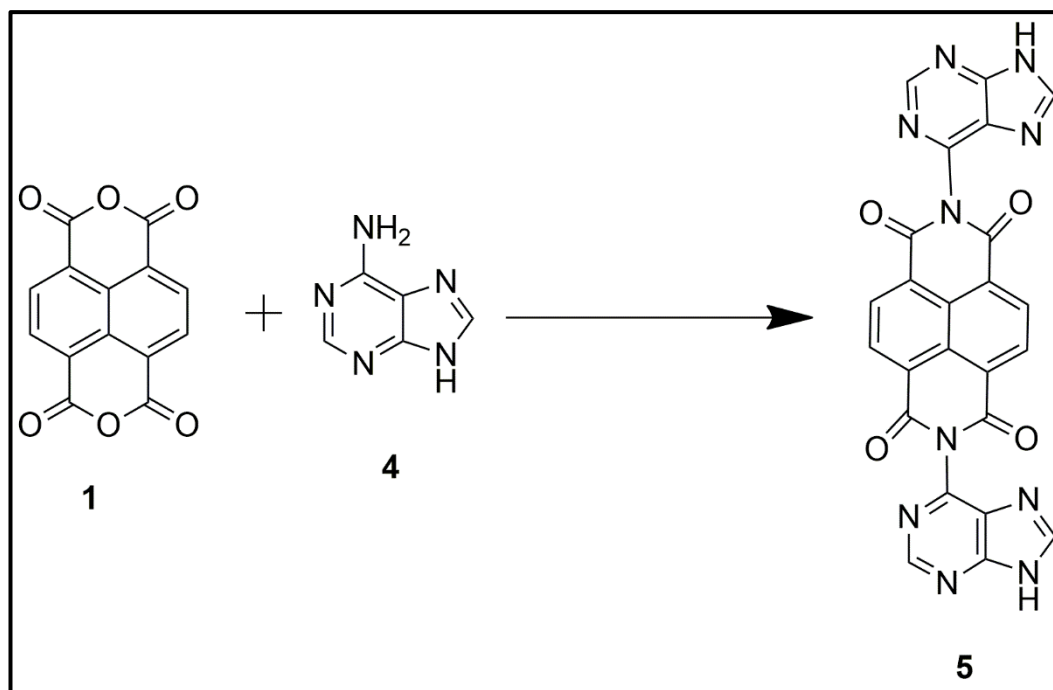
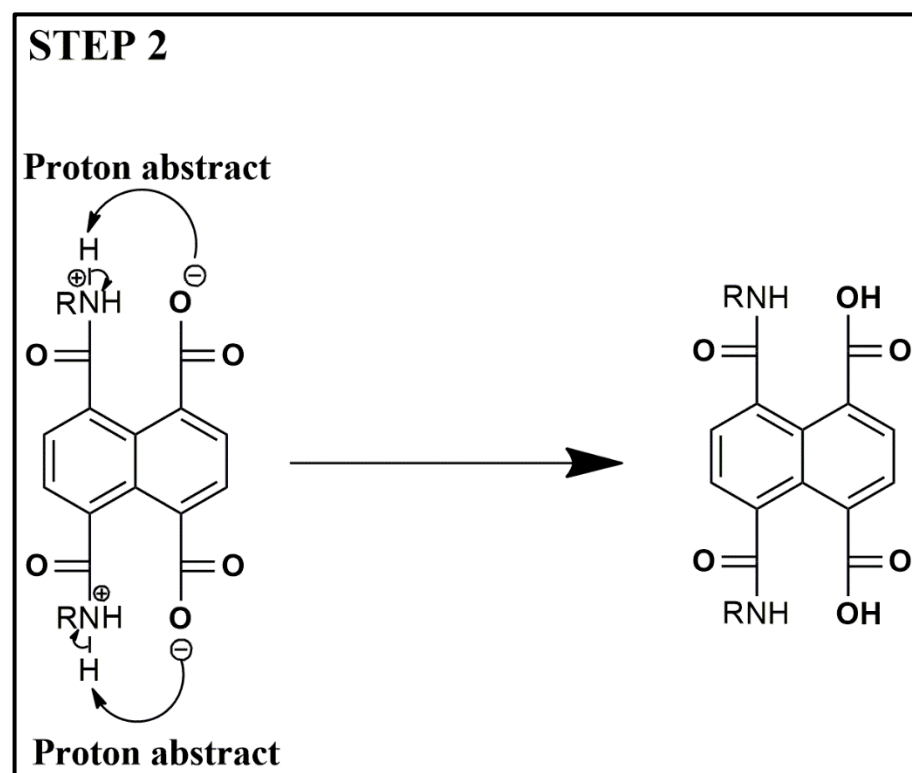
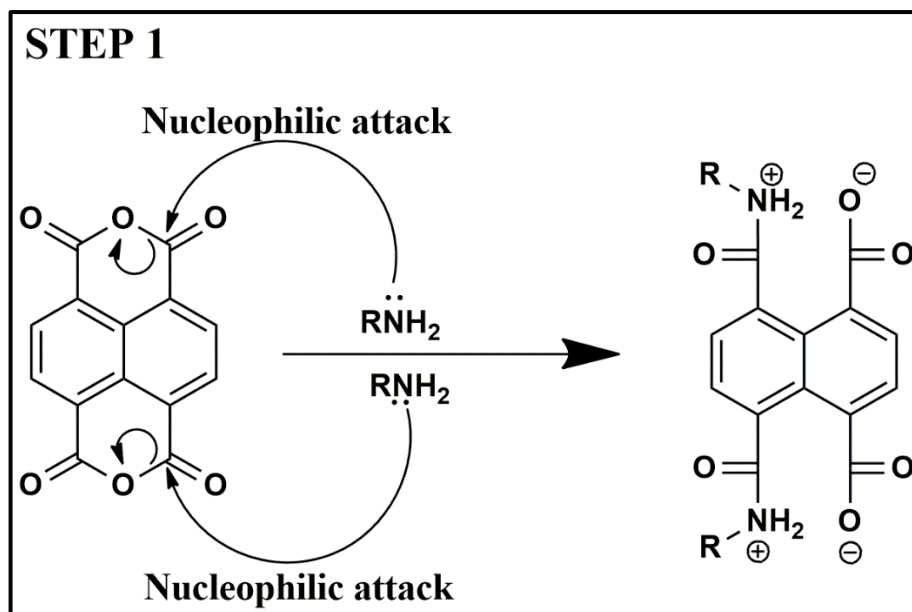
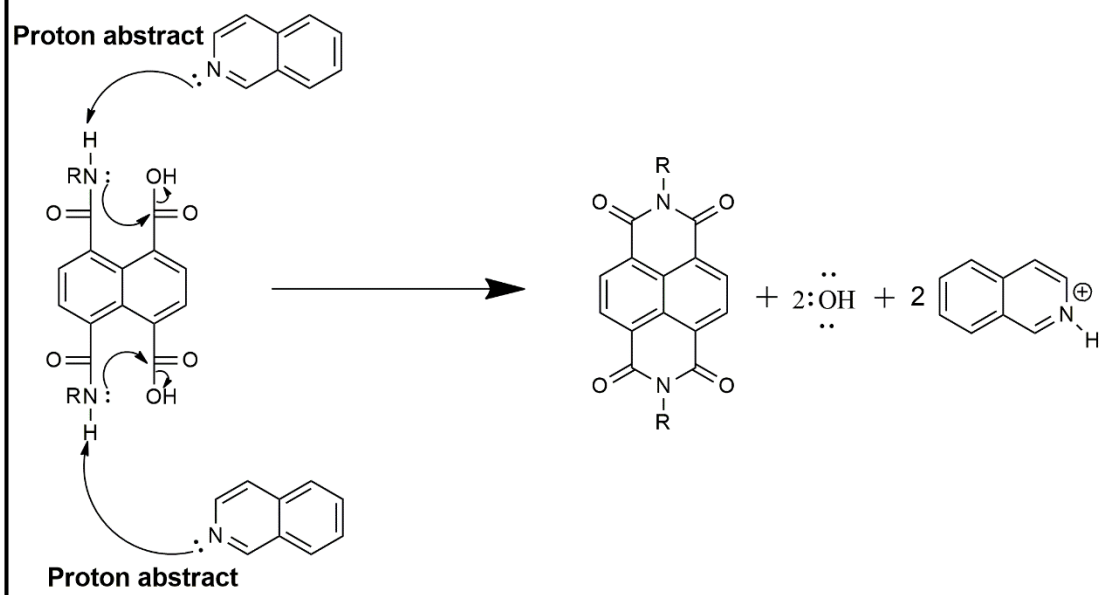


Figure 3.2: Synthesis of N,N'-bis(7H-puriny1)-1,4,5,8-naphthalene diimide (5) from (1) and (4)

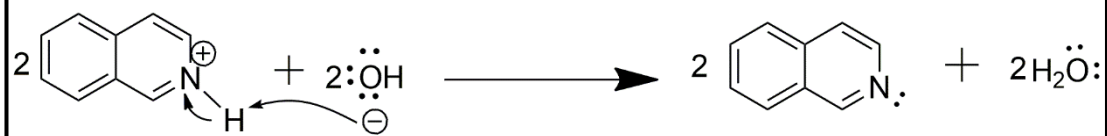
3.3 Mechanism of the Reaction



STEP 3



STEP 4



Chapter 4

DATA AND CALCULATION

4.1 Calculation of Optical Parameters

4.1.1 Molar Absorption Coefficients (ϵ_{\max})

According to the beer lambert's law a linear relation can be seen for absorbance and concentration. Maximum absorption coefficient was measured according to the equation:

$$\epsilon_{\max} = \frac{A}{C \cdot l} \quad (1)$$

ϵ_{\max} Molar absorption coefficient ($\text{L mol}^{-1} \text{cm}^{-1}$)

A Absorbance

C Concentration (mol L^{-1})

l Cell length (cm)

Calculation of ϵ_{\max} for 5:

Five various concentrations were being prepared in order to find ϵ_{\max} . According to their λ_{\max} , their absorbance values were recorded. In the below table their concentration, λ_{\max} absorbance can be seen

Table 4.1: Concentration, maximum wavelength and absorbance for 5 in DMAc

Concentration (M)	λ_{max} (nm)	Absorbance
6.18×10^{-5}	362	0.99
3.09×10^{-5}	362	0.53
1.54×10^{-5}	362	0.28
7.70×10^{-6}	362	0.16
3.86×10^{-6}	362	0.08

As it can be seen from the below graph between concentration and absorbance, their slope equals to the ϵ_{max} .

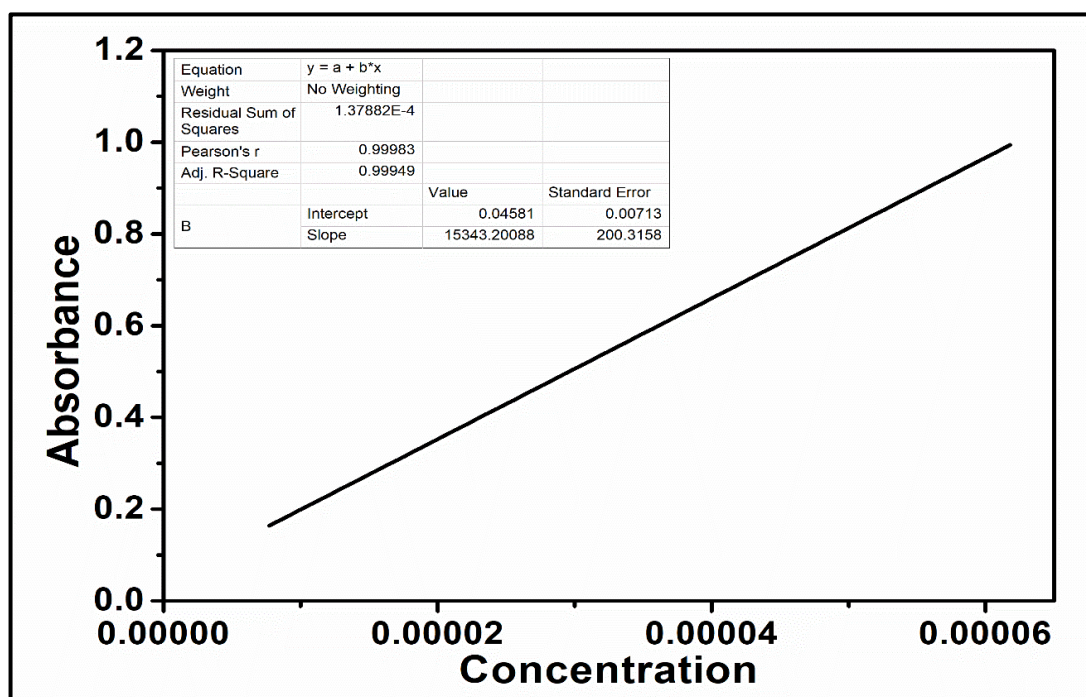


Figure 4.1: Absorbance Vs. concentration of 5 in DMAc

For 5 in DMAc, the slope, which is similar to the ϵ_{\max} , is equal to 15343 L mol⁻¹ cm⁻¹. In the same way, ϵ_{\max} was calculated for 5 in DMF and NMP and it displays from the bellowing table.

Table 4.2: Molar absorption coefficients of 5 in various solvents

5		
Solvents	λ_{\max} (nm)	ϵ_{\max} (—)
DMAc	362	15343
DMF	368	7406
NMP	370	6543

4.1.2 Half Width of Selected Absorption $\nu_{1/2}$

According to the following equation half width of the synthesized naphthalene diimides have been calculated.

$$\nu_{1/2} = \frac{\nu_1 + \nu_2}{2} \quad (2)$$

We can get ν_1 and ν_2 from the absorption spectra which represents the frequency by unit of cm⁻¹. The difference between them, $\nu_{1/2}$, is the half width of selected absorption by cm⁻¹. Finding of the half-width is vital for the compounds in order to calculate the theoretical radiative for them.

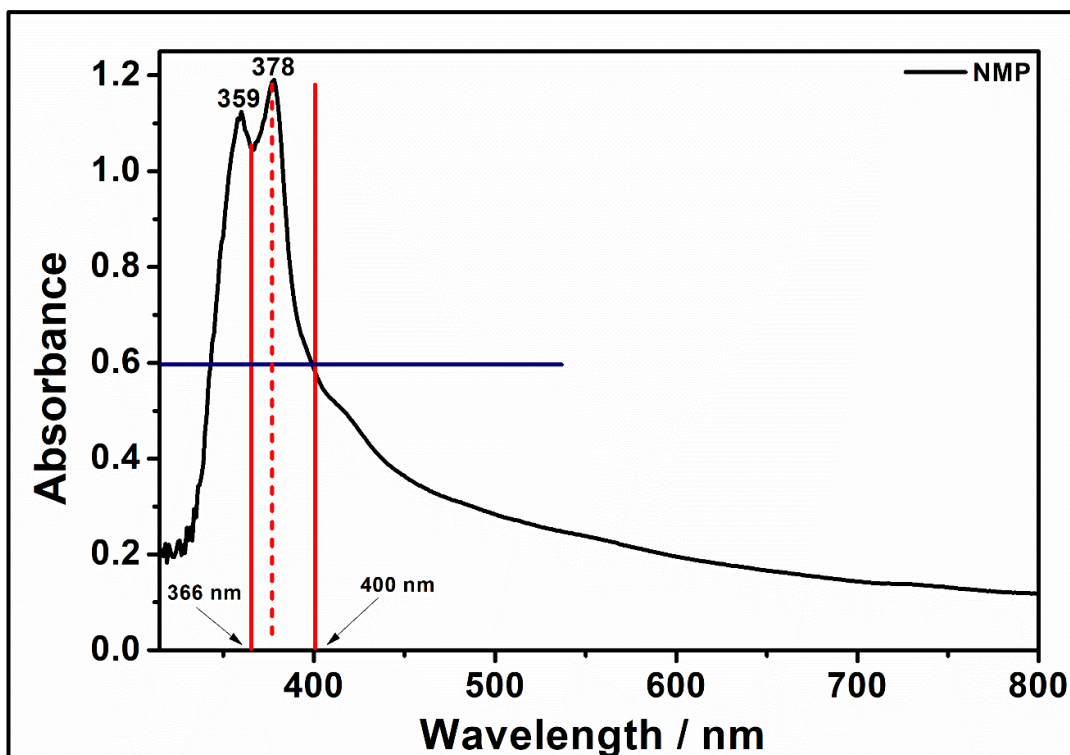


Figure 4.2: Estimation of half width for 3 in NMP

From the Figure 4.2

$$\lambda_1 = 366 \text{ nm}$$

$$\lambda_1 = 366 \text{ nm} \times \frac{1}{10^9} \times \frac{100}{1} = 3.66 \times 10^{-5} \text{ cm}$$

$$\nu_1 = \frac{1}{3.66 \times 10^{-5} \text{ cm}} = 27322 \text{ cm}^{-1}$$

$$\lambda_2 = 400 \text{ nm}$$

$$\lambda_2 = 400 \text{ nm} \times \frac{1}{10^9} \times \frac{100}{1} = 4 \times 10^{-5} \text{ cm}$$

$$\nu_2 = \frac{1}{4 \times 10^{-5} \text{ cm}} = 25000 \text{ cm}^{-1}$$

$$\nu_{1/2} = 27322 - 25000 = 2322 \text{ cm}^{-1}$$

Half width for both compounds are calculated in the same pattern and it can be seen from the table below.

Table 4.3: Half width of 3 and 5 in various solvents

Solvents	Half width $\nu_{1/2}$ (cm^{-1})	
	3	5
DMF	1738	1658
DMAc	2185	2013
DMSO	25063	1634
TFA	24938	2104
Chl	—	1959
NMP	2322	2006

4.1.3 Theoretical Radiative Life Times (τ_0)

Is the lifetime of the excited molecule where there is not radiationless transition. τ_0 for the synthesized 5 was calculated. From Table 4.1, we can find λ_{max} for DMAc and calculate the $\bar{\nu}_{\text{max}}^2$.

$$\lambda_{\text{max}} = 362 \text{ nm} \times \frac{1}{10^9} \times \frac{100 \text{ m}}{1 \text{ m}} = 3.62 \times 10^5 \text{ cm}$$

$$\bar{\nu}_{\text{max}} = \frac{1}{3.62 \times 10^5 \text{ cm}} = 27624 \text{ cm}^{-1}$$

$$\bar{\nu}_{\text{max}}^2 = (27624)^2 = 7.6 \times 10^8 \text{ cm}^{-2}$$

According to the following equations, (τ_0) for 5 in DMAc, DMF and NMP were being calculated.

$$\tau_0 = \frac{3.8 \times 10^8}{2\pi a \times \epsilon_{\text{max}} \times \bar{\nu}_{1/2}^2} \quad (3)$$

τ_0 Theoretical radiative life time (ns)

$\bar{\nu}_{\text{max}}^2$ Mean frequency of λ_{max} (cm^{-1})

ϵ_{max} Maximum extinction coefficient at λ_{max}

$\lambda_{1/2}$ Half width (cm⁻¹)

Theoretical radiative life time of 5 in DMAc:

$$\tau_0 = \frac{3.5 \times 10^8}{(2.76 \times 10^4)^2 \times 15343} = 1.485 \times 10^{-8}$$

$$1.485 \times 10^{-8} \text{ s} \times \frac{10^9}{1} = 14.85$$

For other two solvents, τ_0 was calculated in the same pattern and the result of them were listed in the following table.

Table 4.4: Theoretical radiative life-time (ns) of 5

5					
Solvents	λ_{max} (nm)	ϵ_{max} (L mol ⁻¹ cm ⁻¹)	λ_{max} (nm)	ϵ_{max} (L mol ⁻¹ cm ⁻¹)	τ_0 (ns)
DMAc	362	15343	362	7.6×10^4	14.58
DMF	368	7406	368	7.4×10^4	38.6
NMP	370	6543	370	7.3×10^4	36.5

4.1.4 Calculation of Fluorescence Rate Constant (K_f)

K_f is the speed of emitting of the radiation of molecule. The Fluorescence Rate Constant for the 5 are calculated according to the equation given below

$$K_f = \frac{1}{\tau_0} \quad (4)$$

K_f Fluorescence Rate Constant in s⁻¹

τ_0 Theoretical radiative life-time in s

Theoretical Fluorescence Rate Constant for 5 in DMAc:

$$K_f = \frac{1}{1.485 \times 10^{-8}} = 6.7 \times 10^7 \text{ s}^{-1}$$

For 5 in various solvents were being calculated in the same pattern and displayed in the table below.

Table 4.5: Theoretical fluorescence rate constant for 5 in various solvents

Solvents	$K_f (s^{-1}) (\times 10^7)$
DMAC	6.7
DMF	3.0
NMP	2.7

4.1.5 Oscillator Strength (f)

The strength of the electronic transition is displayed by the oscillator strength, which is dimensionless. By the following equation, f for the prepared naphthalene diimides was calculated.

$$f = 4.32 \times 10^{-9} \times \nu_{1/2}^2 \times \epsilon_{\max} \quad (5)$$

f Oscillator strength

$\nu_{1/2}$ Half width of selected absorption (cm^{-1})

ϵ_{\max} Maximum Extinction Coefficients in $\text{L. mol}^{-1} \cdot \text{cm}^{-1}$

Oscillator strength for 5 in DMAc:

$$f = 4.32 \times 10^{-9} \times 2013 \times 15343 = 0.13$$

Table 4.6: Oscillator strength of 5 in various solvents

Oscillator strength (<i>f</i>)	
Solvents	5
DMAC	0.130
DMF	0.053
NMP	0.057

4.1.6 Singlet Energies (E_s)

Singlet energy can be defined as the least amount of energy which is required to excite a chromophore from ground state to the excited state.

$$E_s = \frac{2.86 \times 10^5}{\lambda_{\max}} \quad (6)$$

E_s Singlet energy in (Kcal.mol⁻¹)

λ_{\max} Maximum absorption wavelength Å

Singlet energies of 5 in DMAc

$$\lambda_{\max} = 362 \text{ nm} \times \frac{10}{1} = 3620 \text{ Å}$$

$$E_s = \frac{2.86 \times 10^5}{3620} = 79 \text{ Kcal.mol}^{-1}$$

Table 4.7: Singlet energies of 5 in various solvents

Solvents	λ_{max} (Å)	Es (Kcal.mol ⁻¹)
DMAc	3620	79
DMSO	3690	77.5
DMF	3680	77.7
TFA	3620	79
CHL	3650	78.4
NMP	3700	77.3

Table 4.8: Singlet energies of 3 in various solvents

Solvents	λ_{max} (Å)	Es (Kcal.mol ⁻¹)
DMAc	3770	71.1
DMSO	3790	75.5
DMF	3770	75.9
TFA	3810	75.01
CHL	—	—
NMP	3780	75.7

Table 4.9: Photophysical properties of and 5 in various solvents

5							
Solvents	λ_{\max}	ϵ_{\max}	$\tilde{\nu}_{1/2}$	τ_0	K_f	f	Es
DMAc	362	15343	2013	14.58	6.7	0.130	79
DMF	368	7406	1658	38.6	3.0	0.053	77.7
NMP	370	2006	2006	36.5	2.7	0.057	77.3

Maximun absorption wavelength λ_{\max} (nm), molar absorption coefficients ϵ_{\max} (L.mol⁻¹.cm⁻¹), Oscillator strength f , radiative lifetime τ_0 (ns), fluorescence rate constant K_f (10⁷ s⁻¹), singlet energy Es (Kcal.mol⁻¹) and half width $\tilde{\nu}_{1/2}$ cm⁻¹.

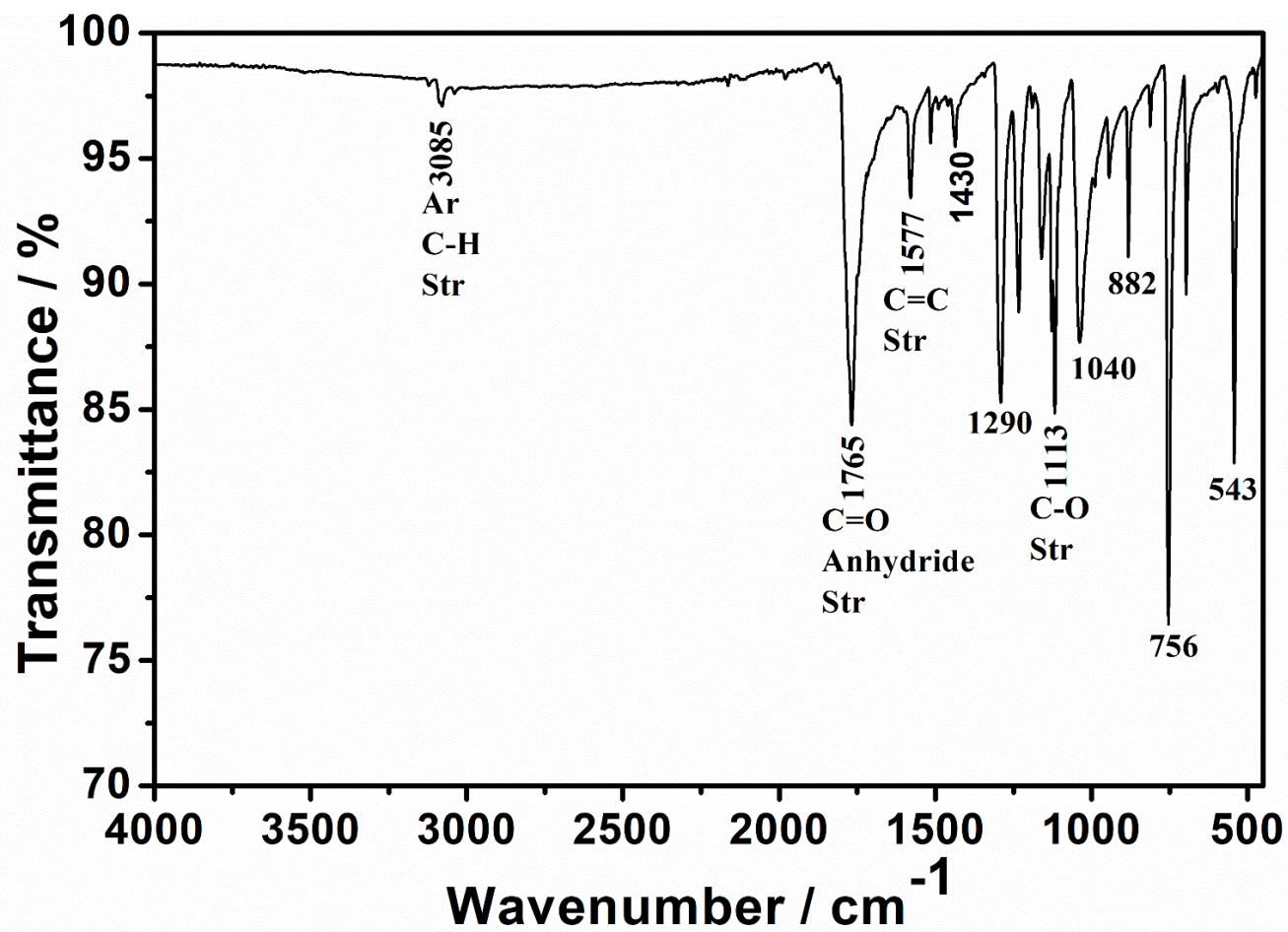


Figure 4.3: FT-IR spectrum of 1,4,5,8- Naphthalenetetracarboxylic dianhydride

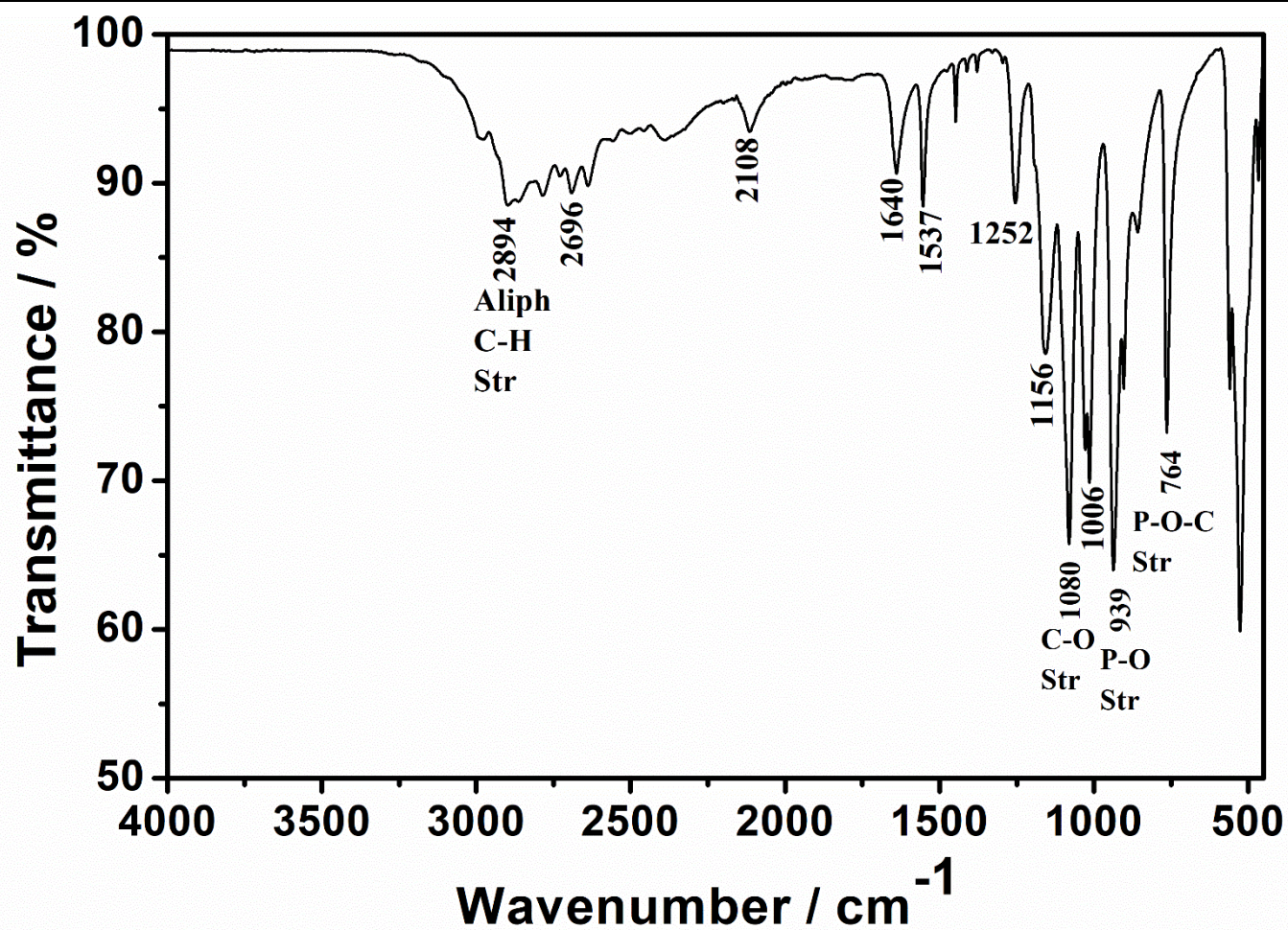


Figure 4.4: FT-IR spectrum of 2-aminoethyl dihydrogen phosphate, amine (2)

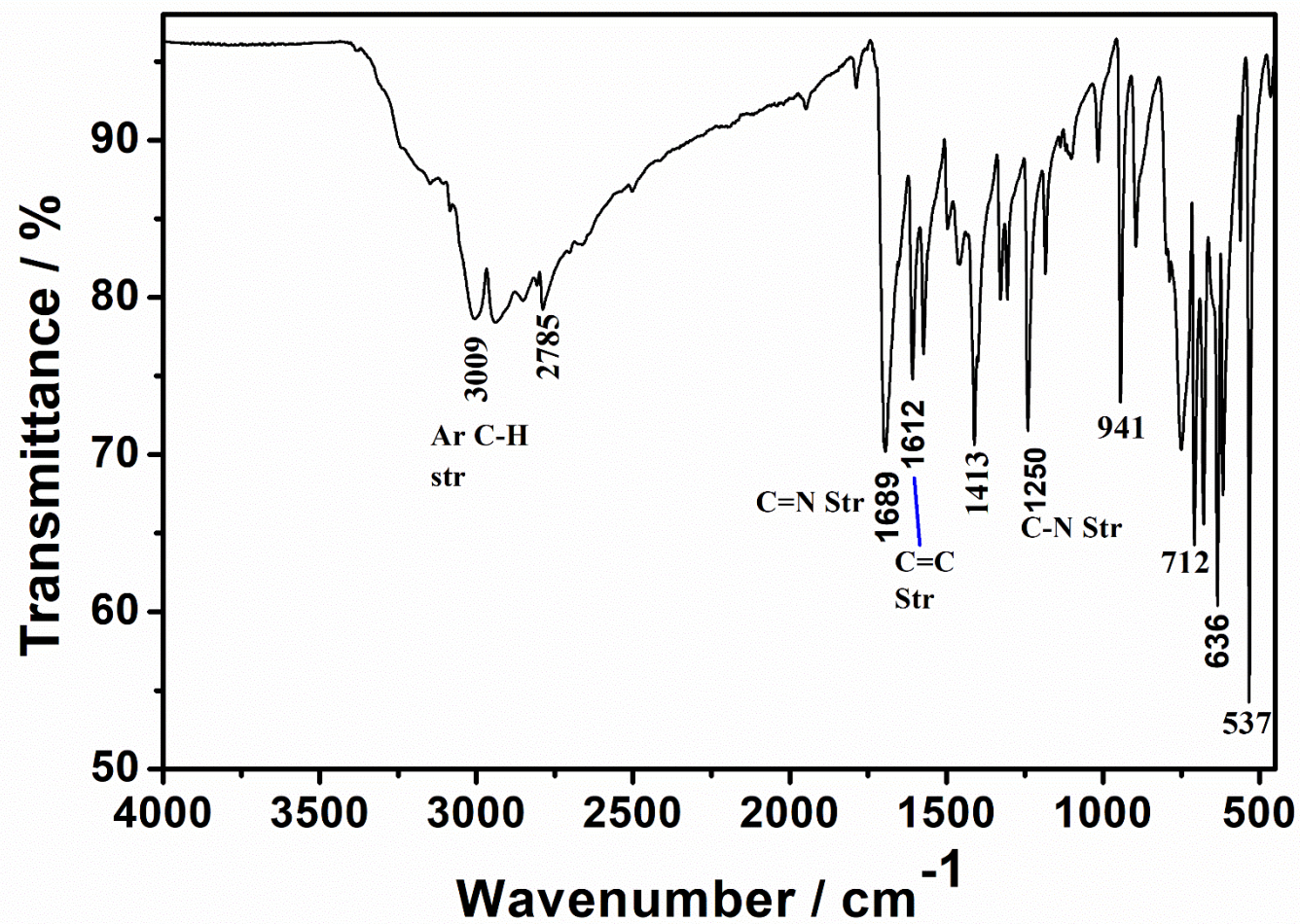


Figure 4.5: FT-IR spectrum of 7H-purine-6-amine, amine (4)

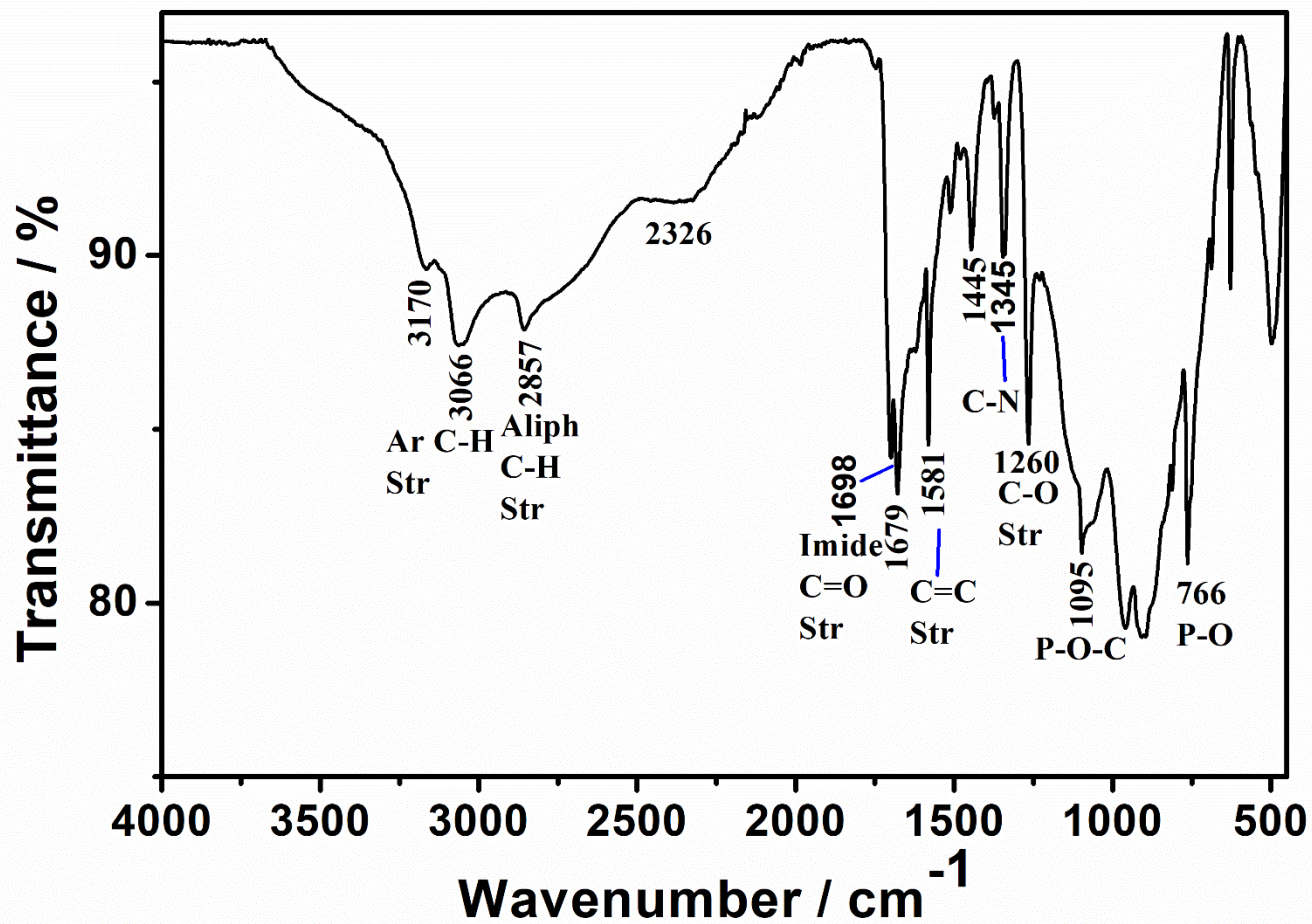


Figure 4.6: FT-IR spectrum of N,N'-bis[(2-(dihydrogenphosphoryl)ethyl)]-1,4,5,8-naphthalene diimide

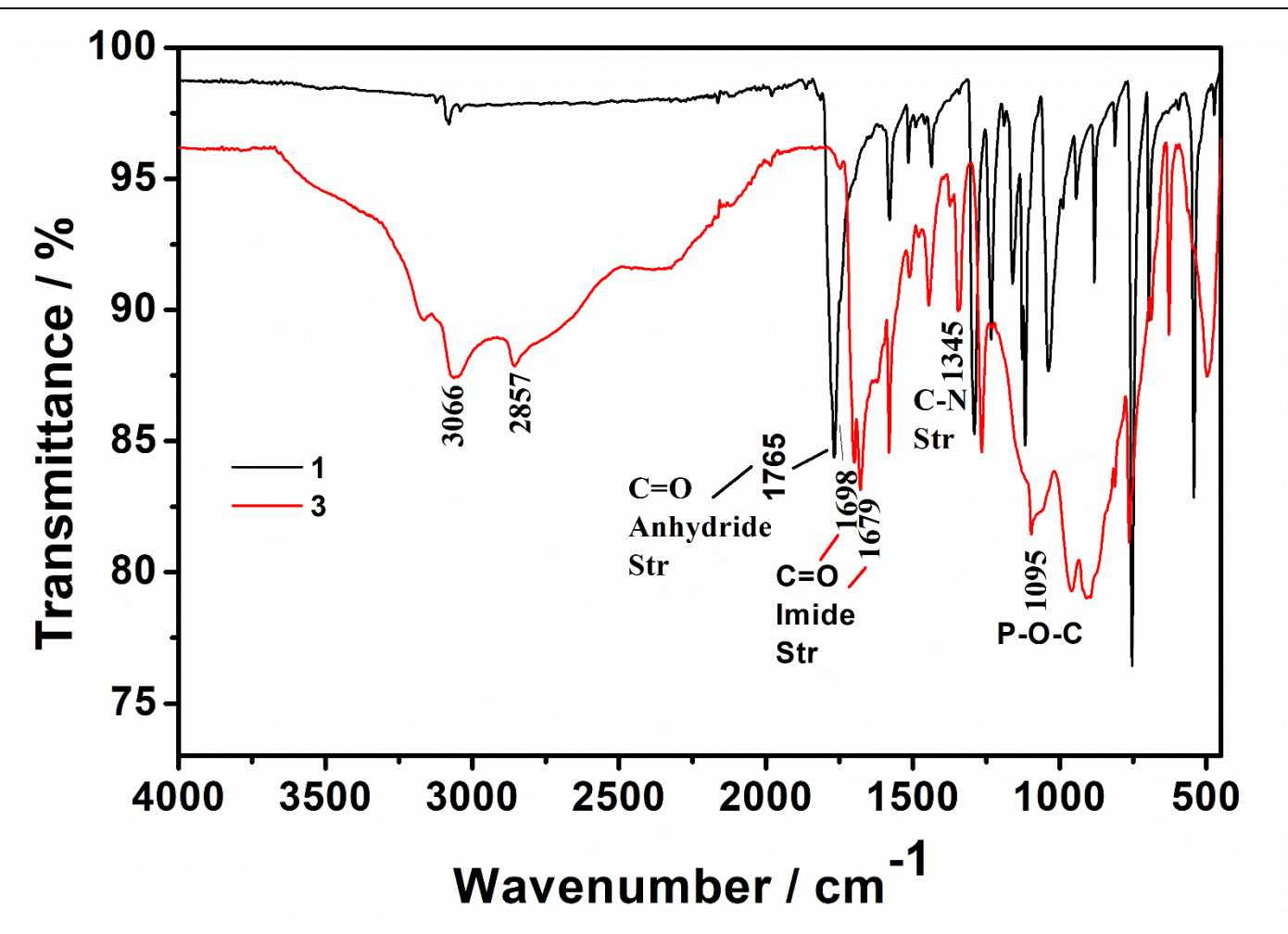


Figure 4.7: FT-IR spectrum of 1 and 3

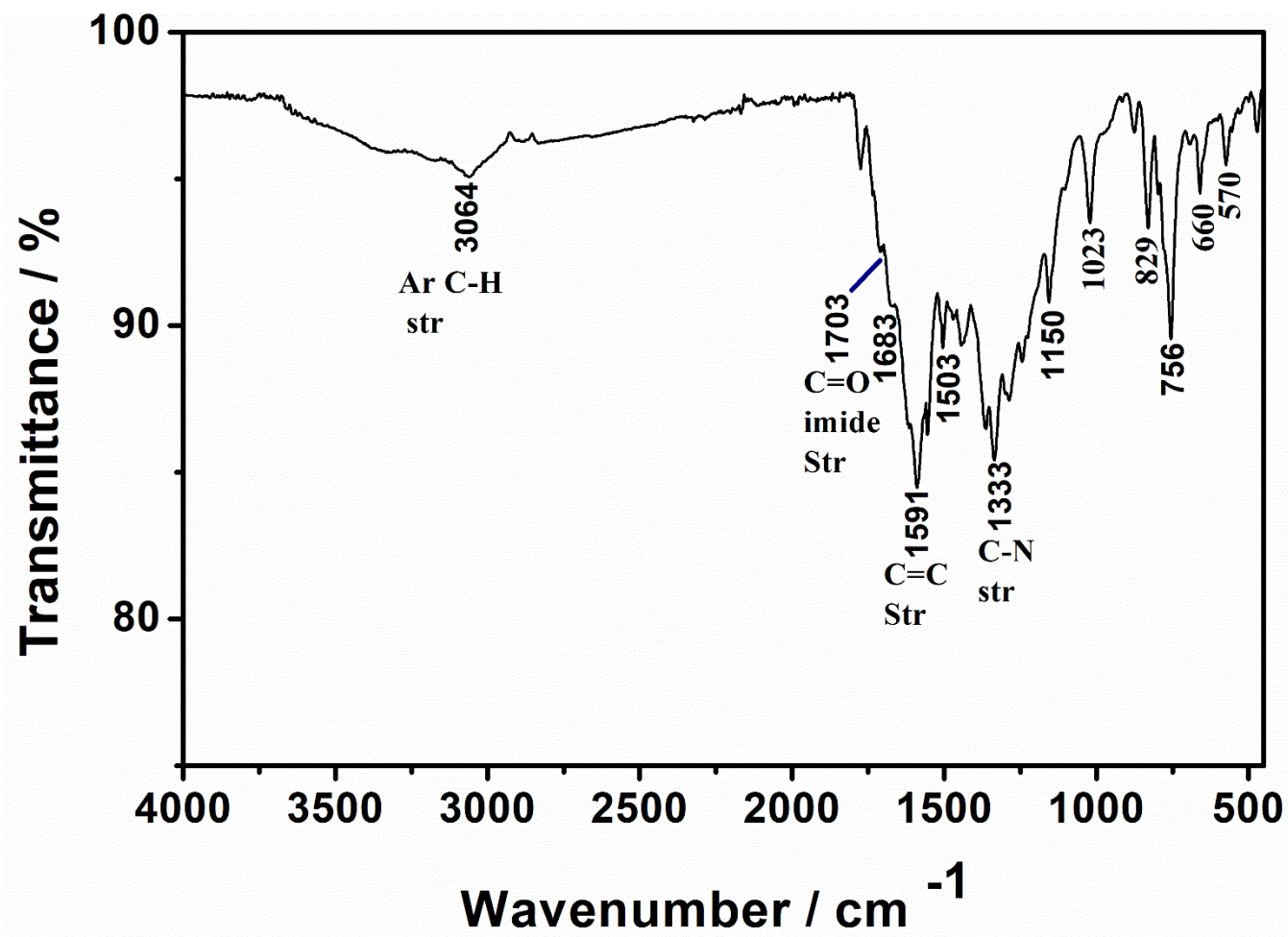


Figure 4.8: FT-IR spectrum of N,N'-bis(7H-purinyl)-1,4,5,8-naphthalene diimide

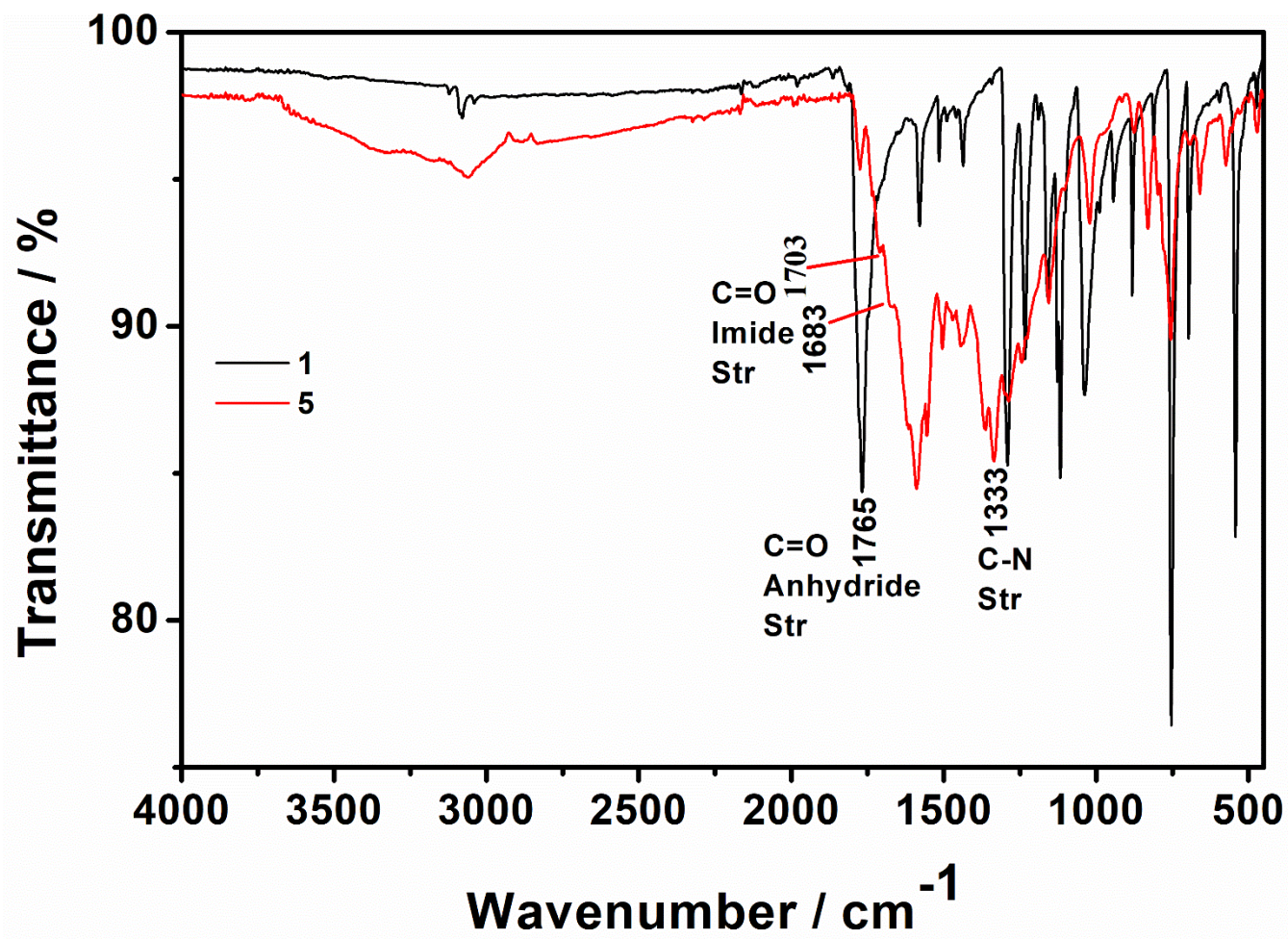


Figure 4.9: FT-IR spectrum of 1 with 5

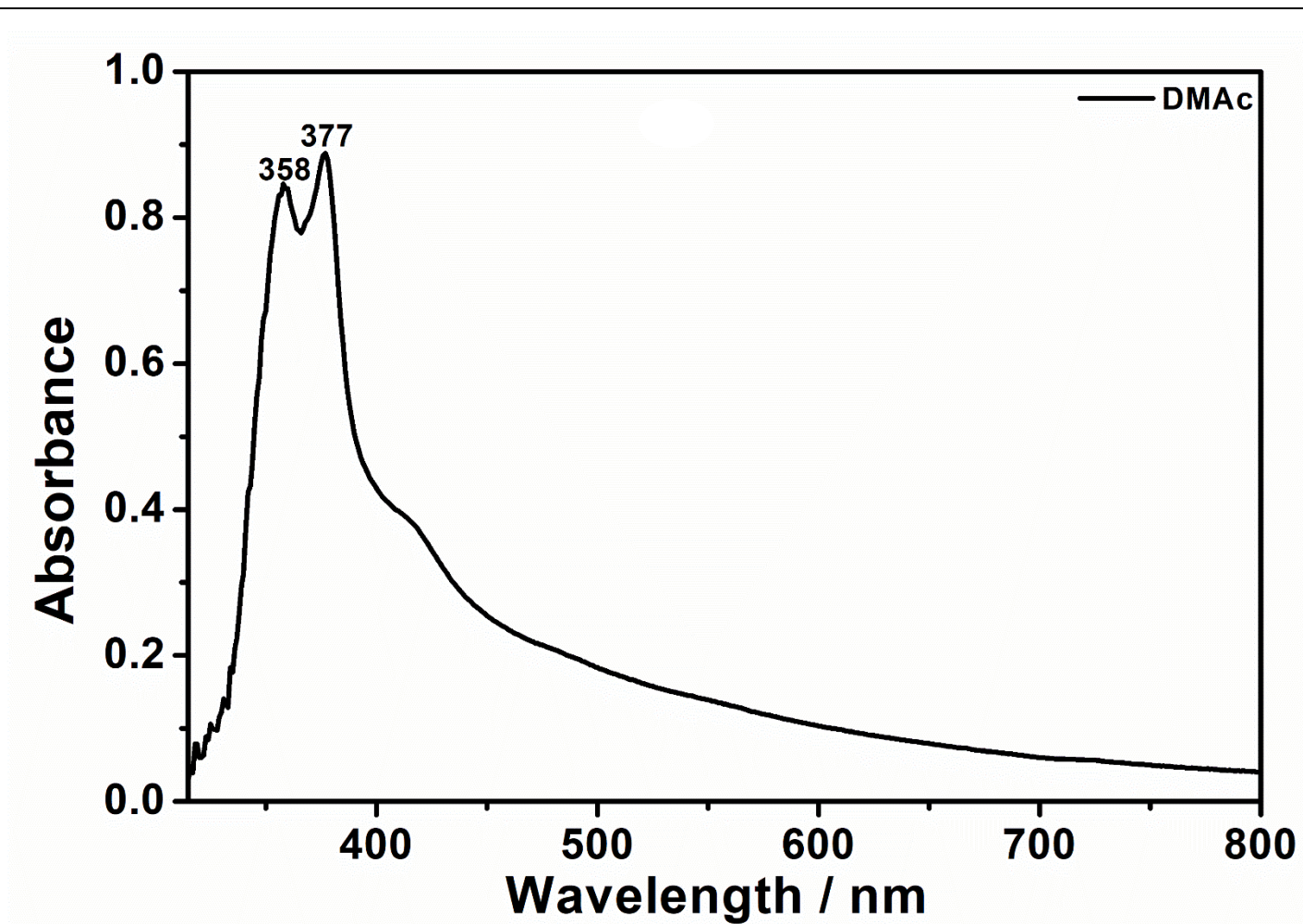


Figure 4.10: UV / Vis spectrum of N,N'-bis[(2-(dihydrogenphosphoryl)ethyl)]-1,4,5,8-naphthalene diimide in DMAc

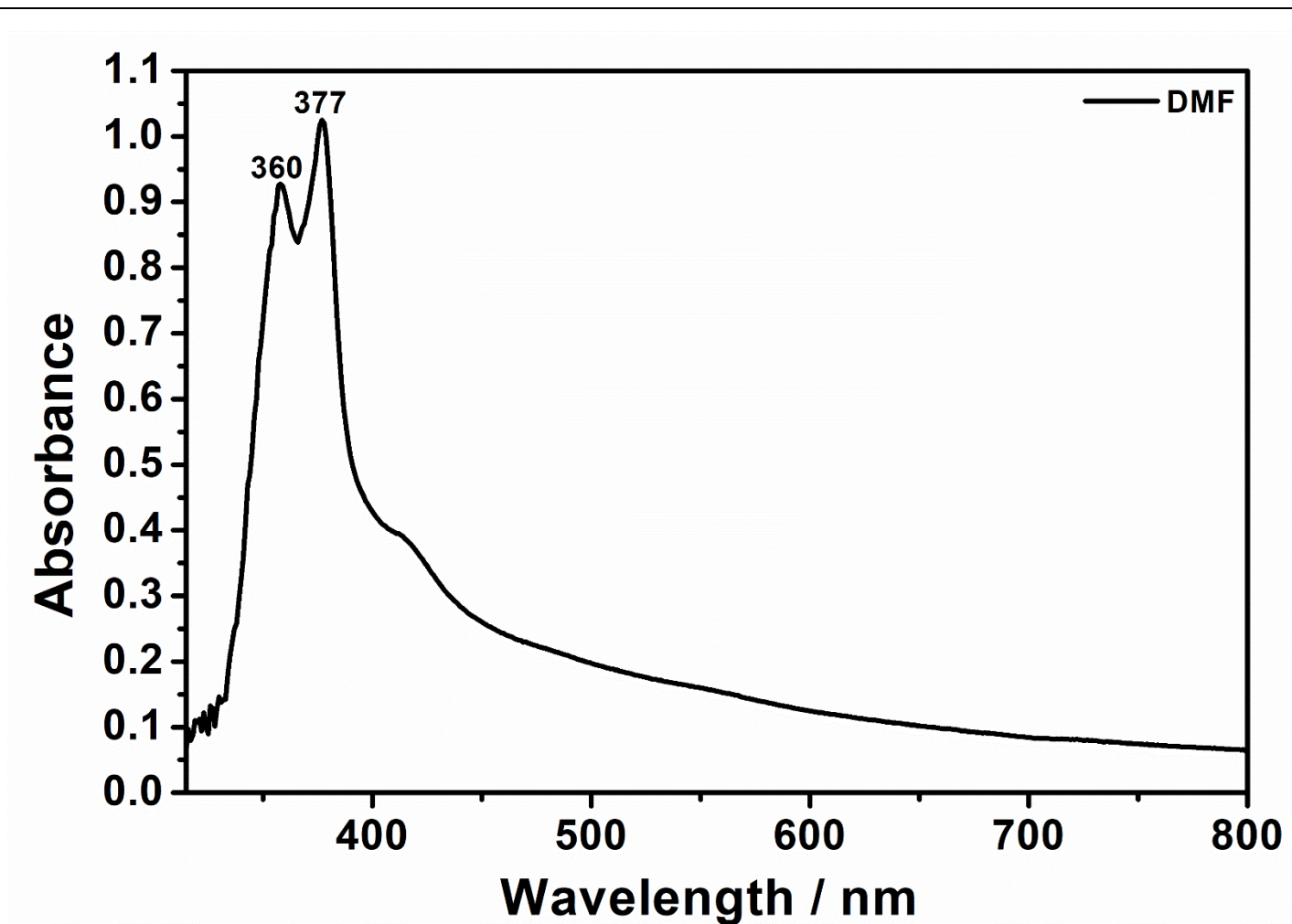


Figure 4.11: UV / Vis spectrum of N,N'-bis[(2-(dihydrogenphosphoryl)ethyl)]-1,4,5,8- naphthalene diimide in DMF

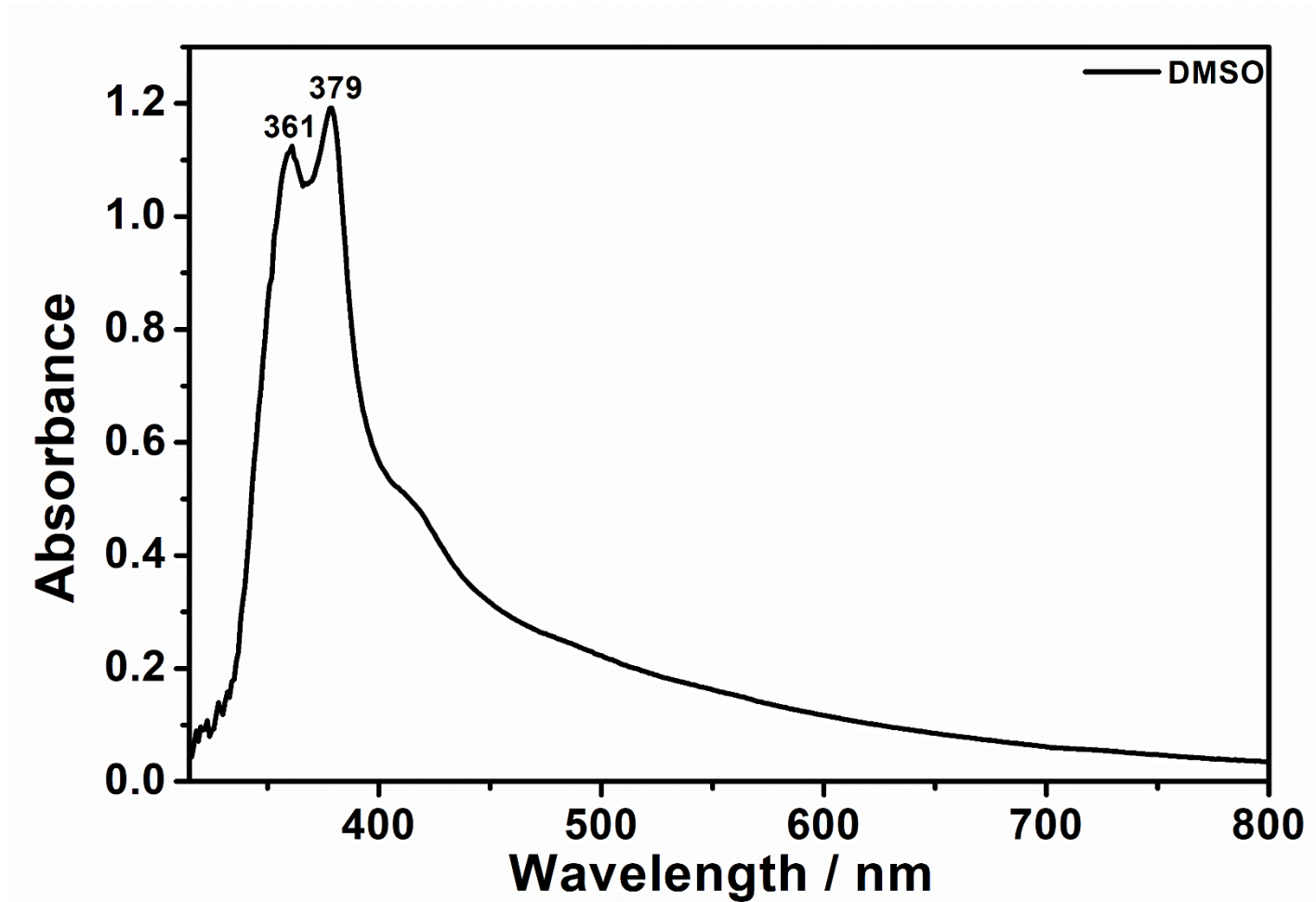


Figure 4.12: UV / Vis spectrum of N,N'-bis[(2-(dihydrogenphosphoryl)ethyl)]-1,4,5,8-naphthalene diimide in DMSO

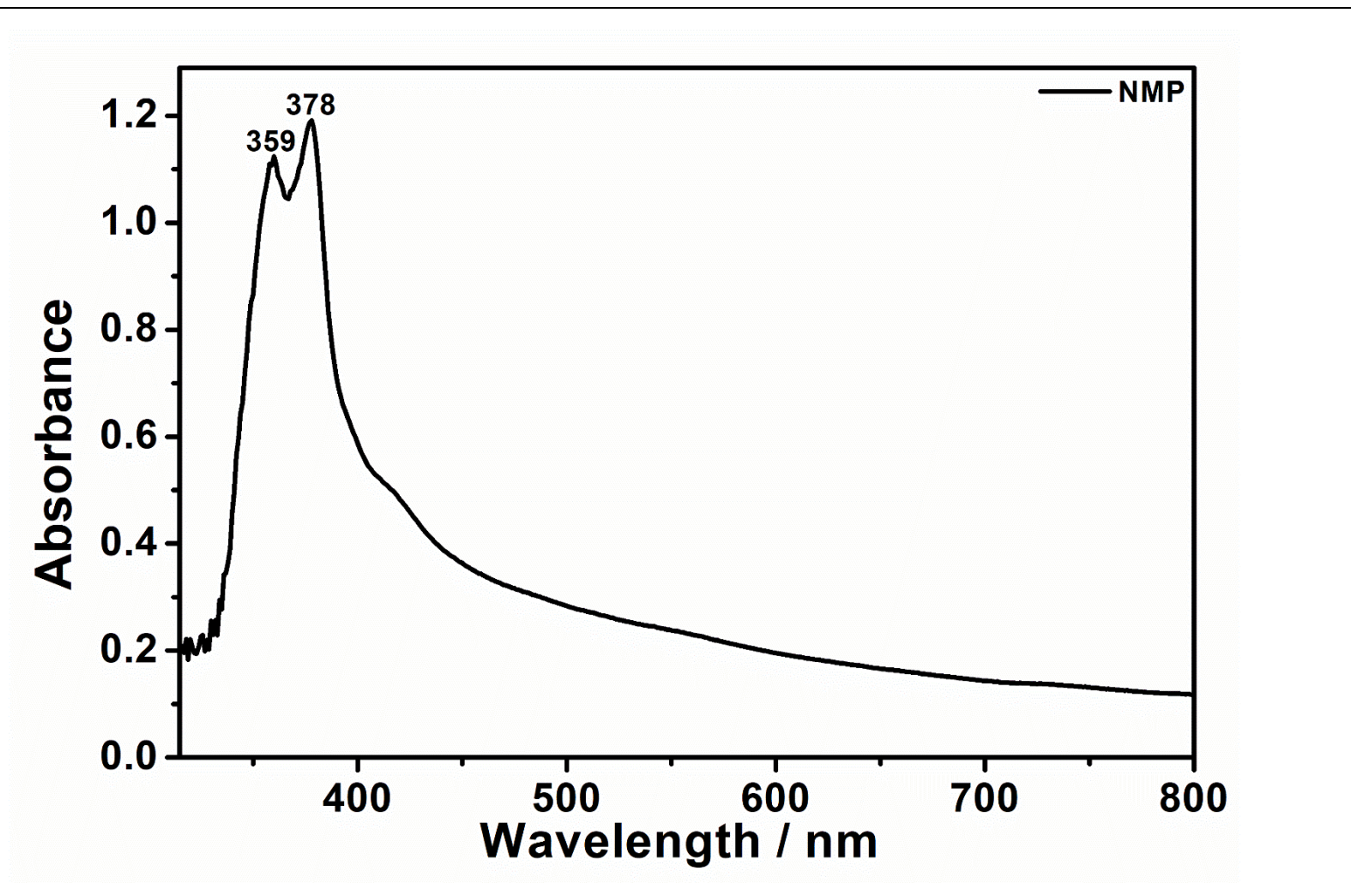


Figure 4.13: UV / Vis spectrum of N,N'-bis[(2-(dihydrogenphosphoryl)ethyl)]-1,4,5,8- naphthalene diimide in NMP

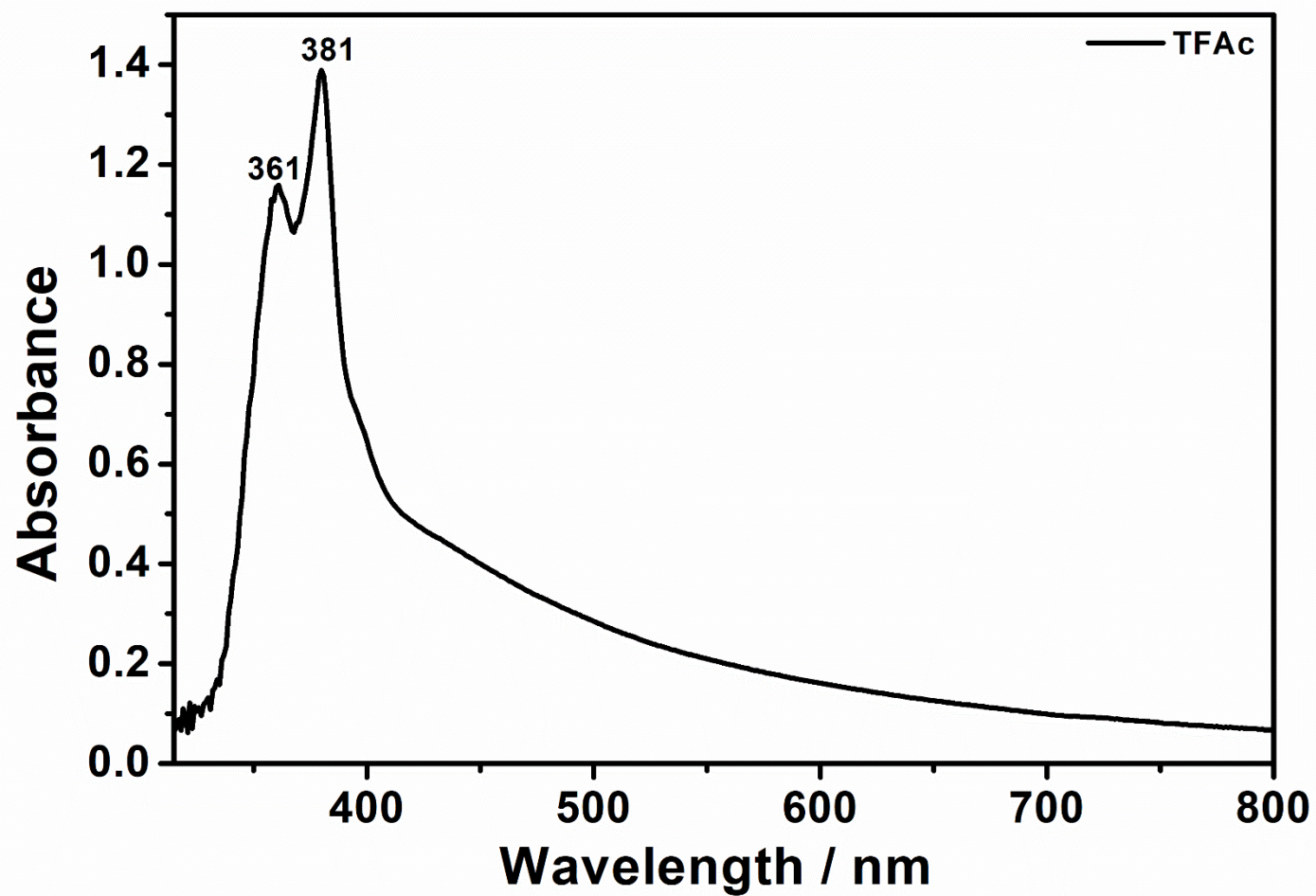


Figure 4.14: UV / Vis spectrum of N,N'-bis[(2-(dihydrogenphosphoryl)ethyl)]-1,4,5,8-naphthalene diimide in TFAc

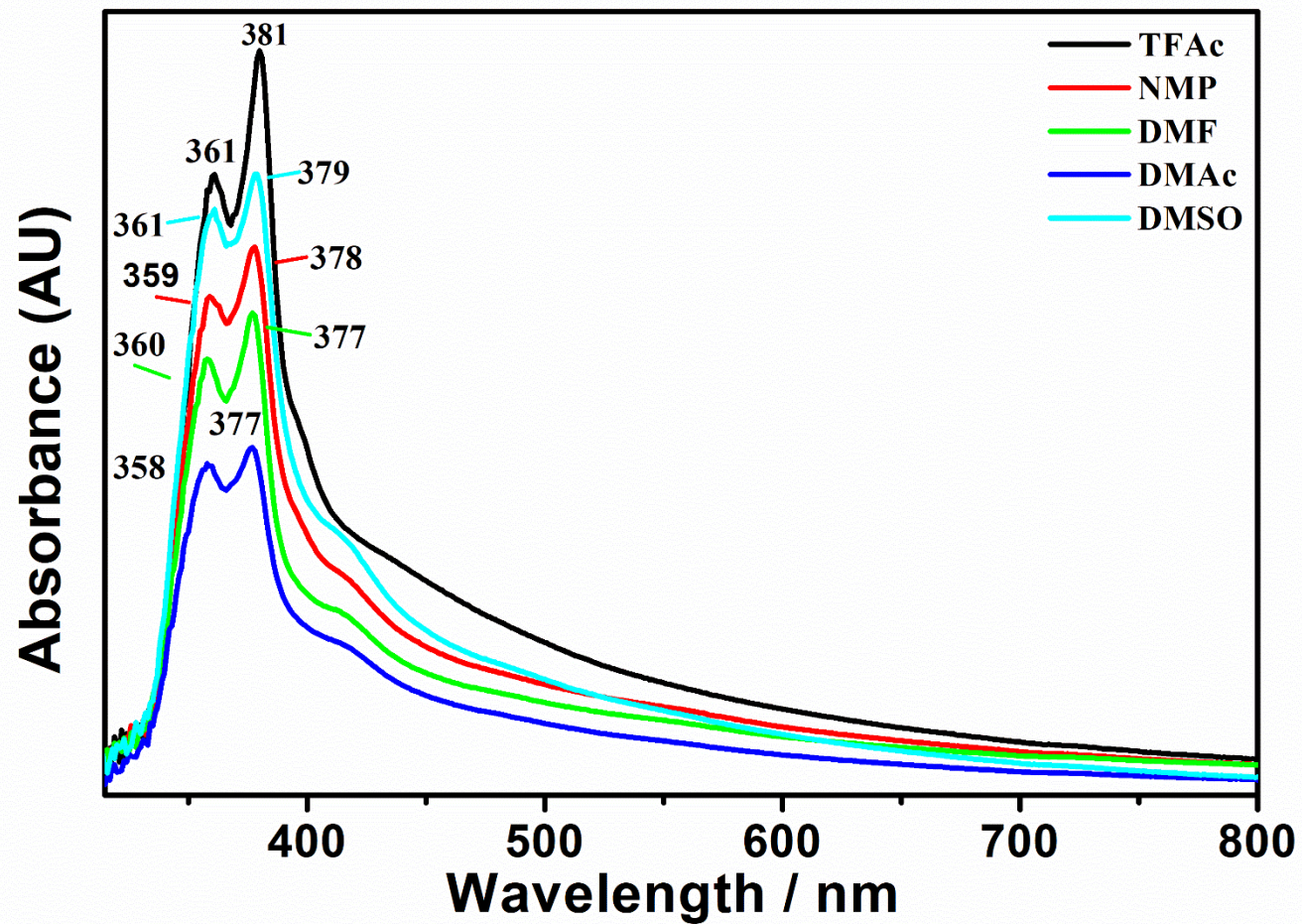


Figure 4.15: UV / Vis spectrum of N,N'-bis[(2-(dihydrogenphosphoryl)ethyl)]-1,4,5,8-naphthalene diimide in various solvents

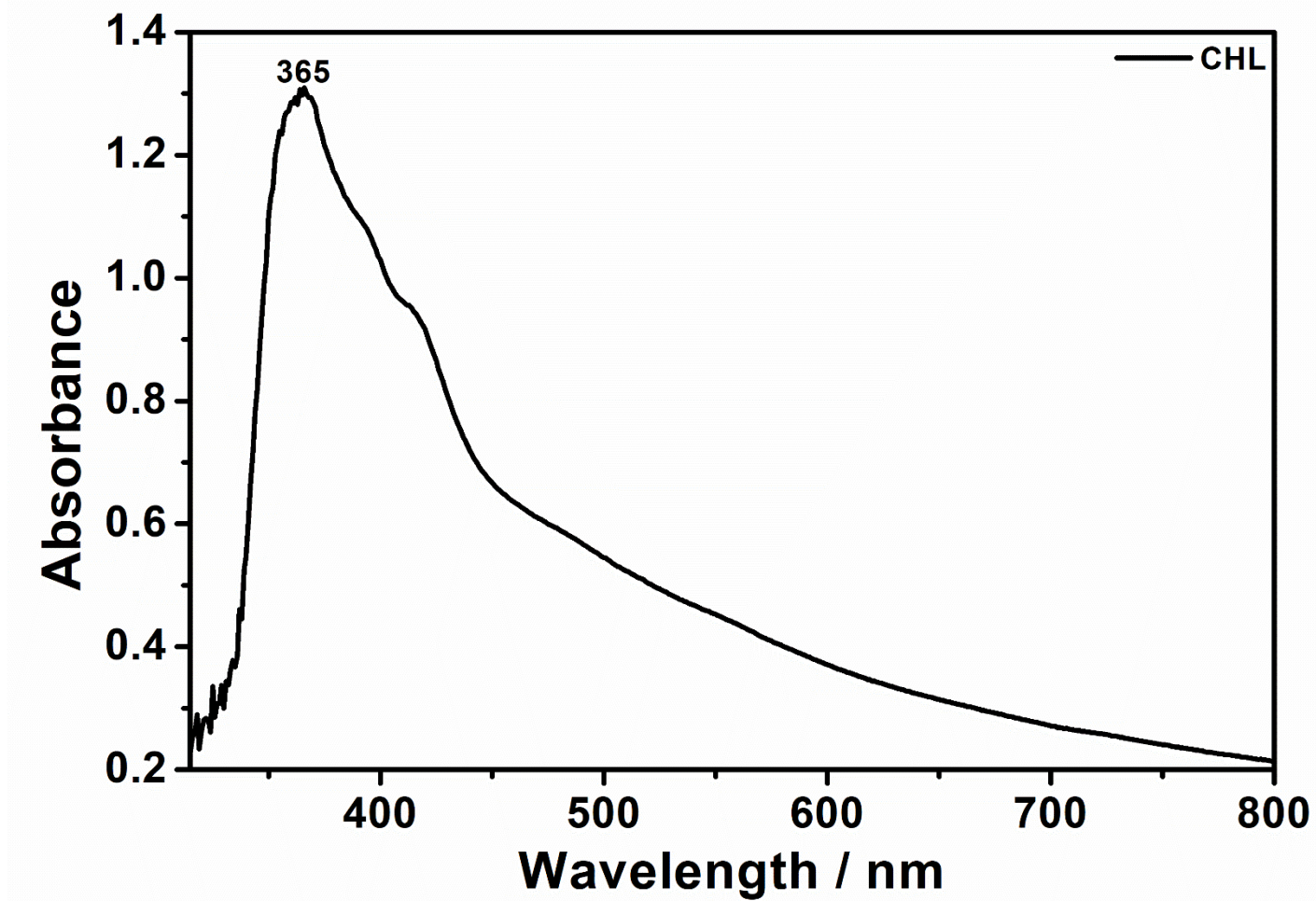


Figure 4.16: UV / Vis spectrum of N,N'-bis(7H-purinyl)-1,4,5,8-naphthalene diimide in CHL

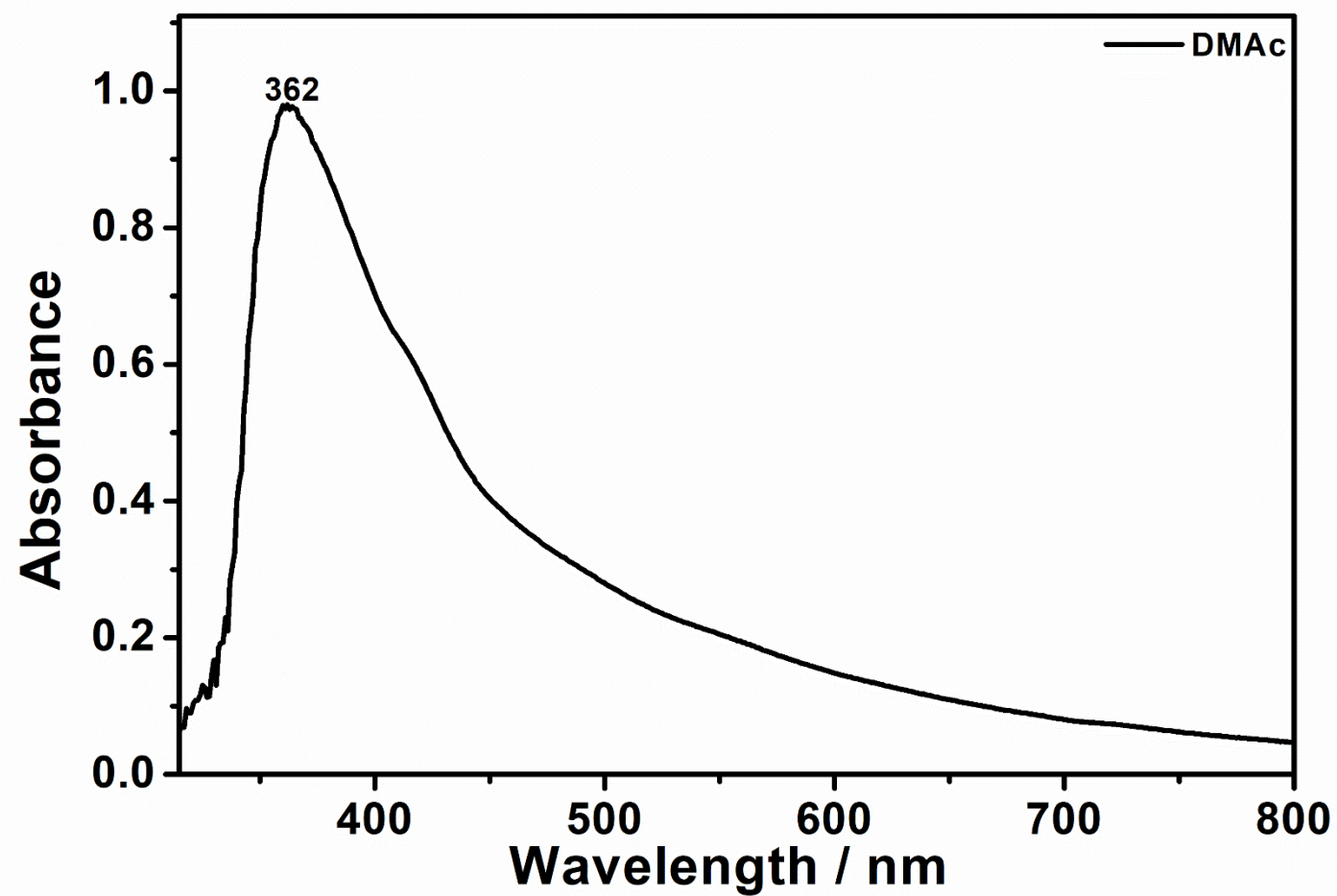


Figure 4.17: UV / Vis spectrum of N,N'-bis(7H-purinyl)-1,4,5,8-naphthalene diimide in DMAc

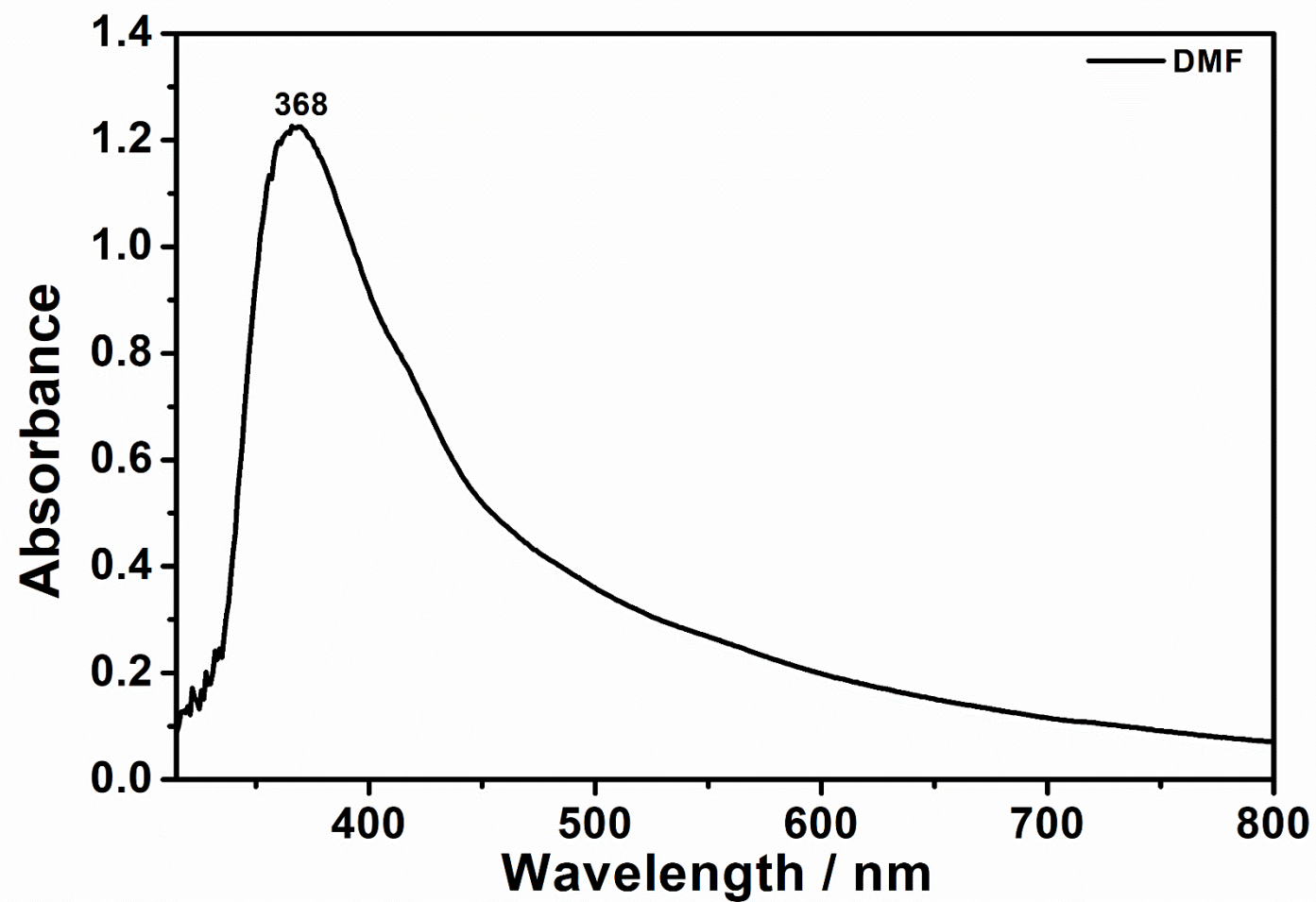


Figure 4.18: UV / Vis spectrum of N,N'-bis(7H-purinyl)-1,4,5,8-naphthalene diimide in DMF

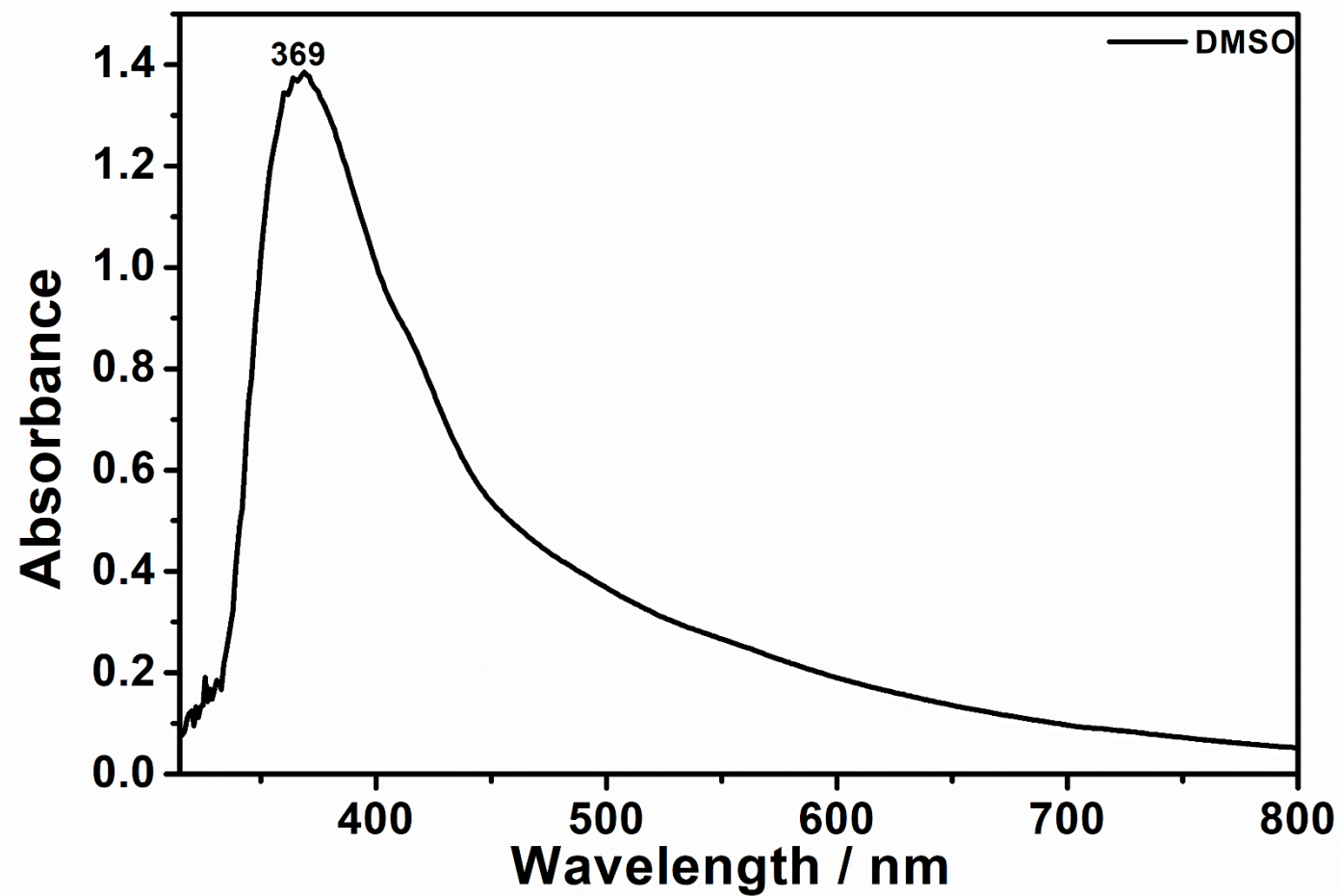


Figure 4.19: UV / Vis spectrum of N,N'-bis(7H-puriny)-1,4,5,8-naphthalene diimide in DMSO

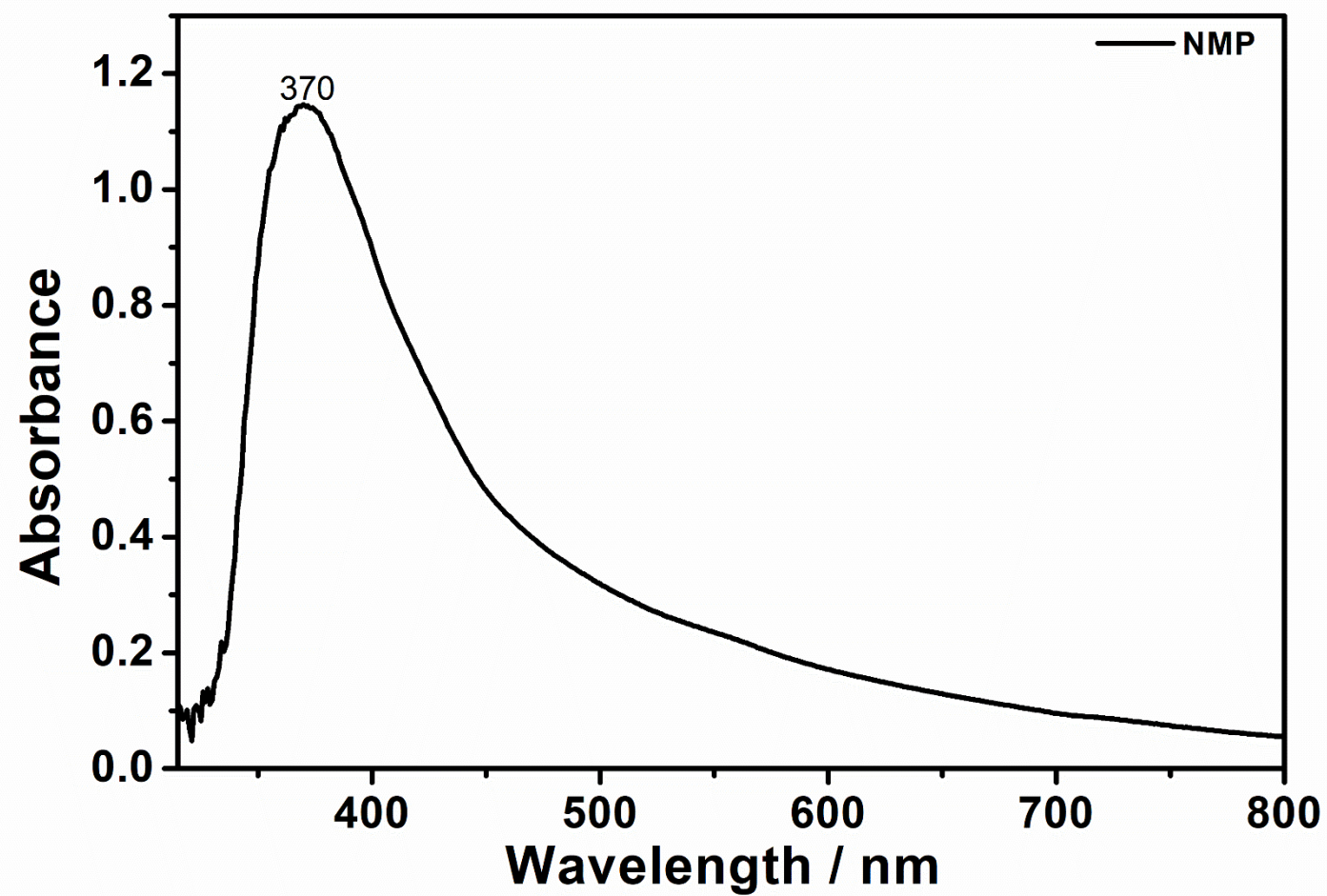


Figure 4.20: UV / Vis spectrum of N,N'-bis(7H-purinyl)-1,4,5,8-naphthalene diimide in NMP

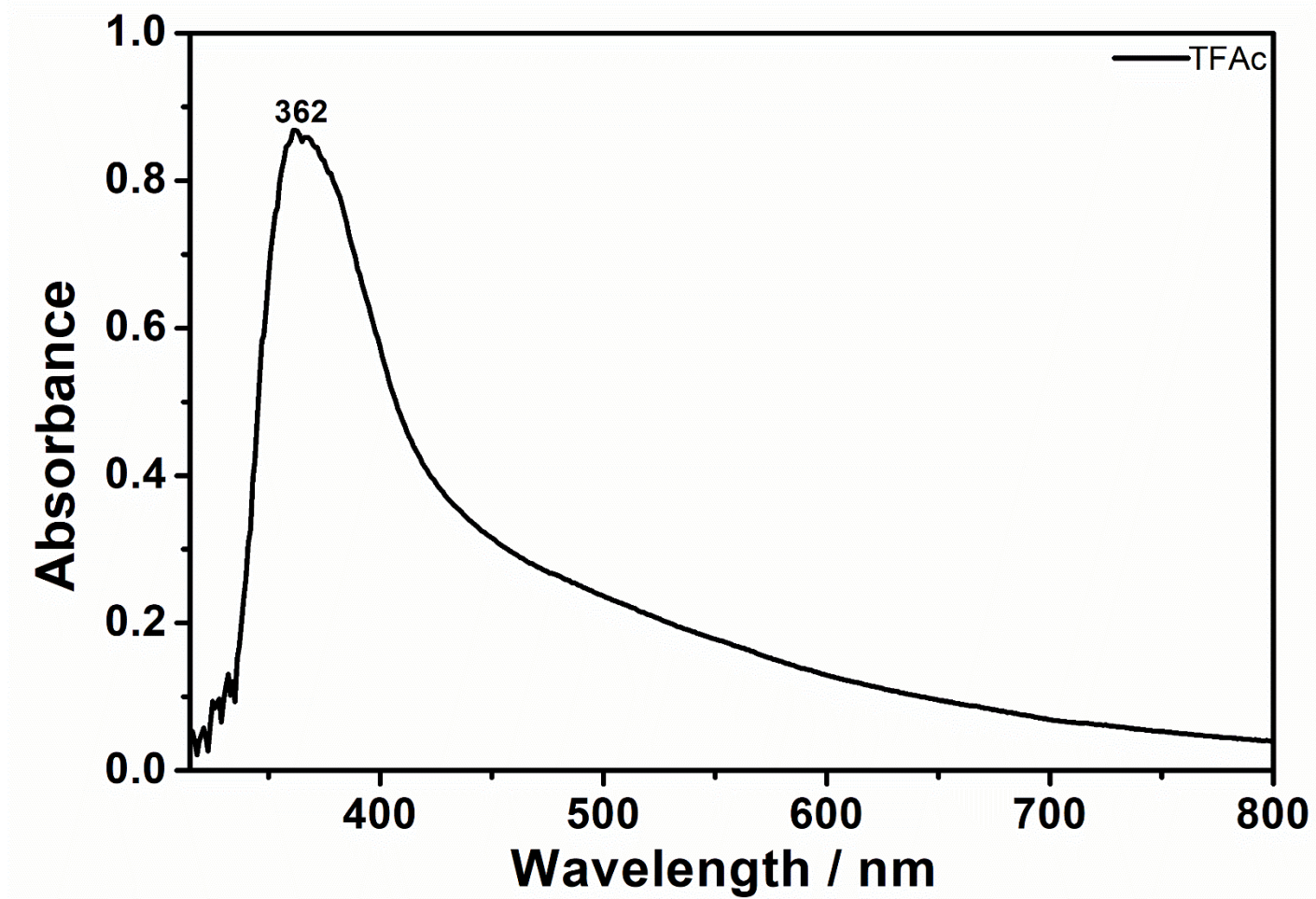


Figure 4.21: UV / Vis spectrum of N,N'-bis(7H-purinyl)-1,4,5,8-naphthalene diimide in TFAc

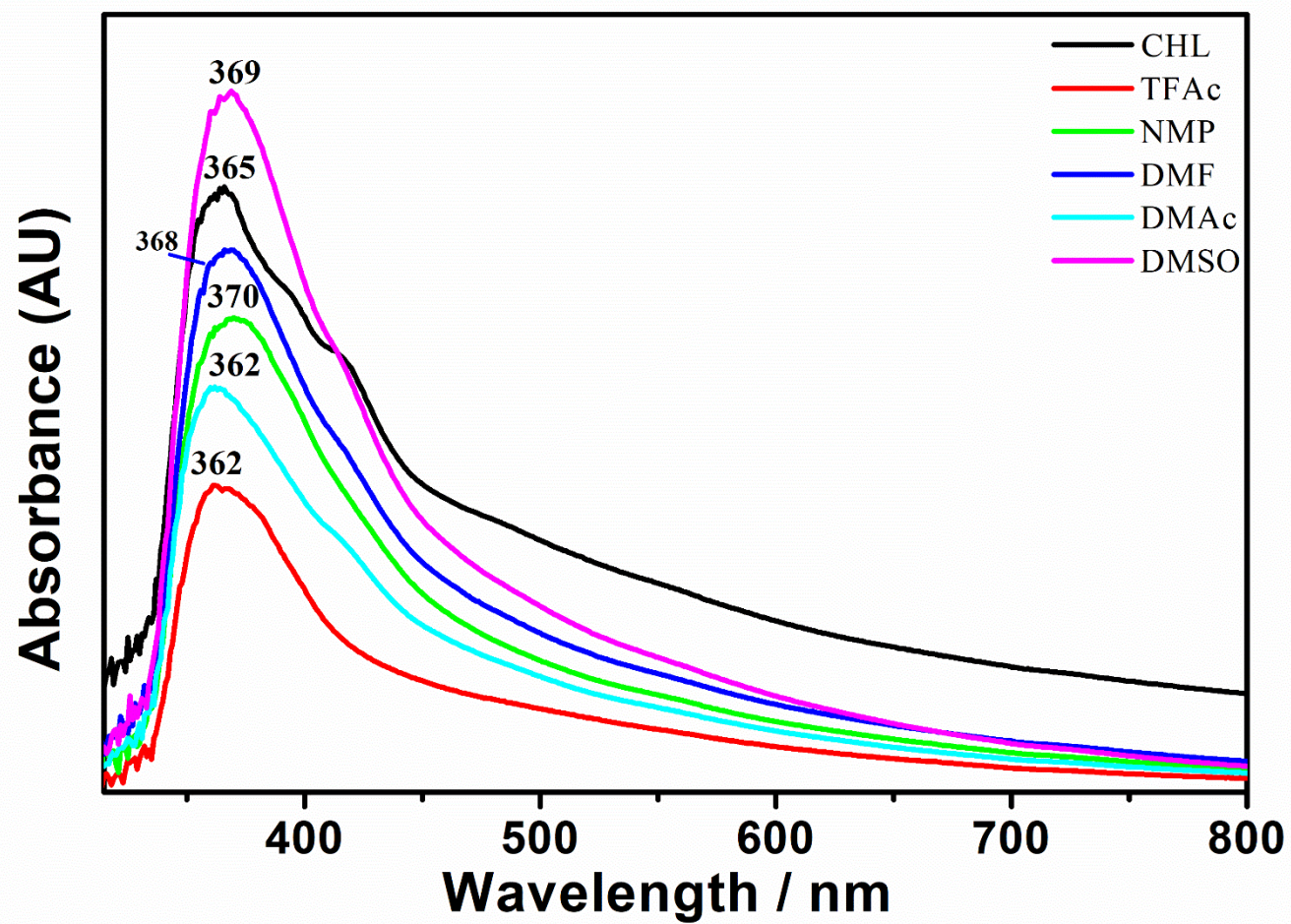


Figure 4.22: UV / Vis spectrum of N,N'-bis(7H-purinyl)-1,4,5,8-naphthalene diimide in various solvents

Chapter 5

RESULTS AND DISCUSSION

5.1 Synthesis of N,N'-bis(2-(dihydrogenphosphoryl)ethyl)-1,4,5,8-naphthalene diimide (3) and IR spectra analysis

N,N'-bis[(2-(dihydrogenphosphoryl)ethyl)]-1,4,5,8-naphthalene diimide (3) was synthesized successfully according to the procedure recorded in the section 3.2.1. Compound 3 was purified by using acetone soxhlet to get rid of high boiling solvents and impurities integrate with the recrystallization technique by using DMSO, which was followed by TLC. The color of the product is black with the yield of 85.5 %.

Analysis of 3 has been done by using FT-IR and it can be seen in the figure 4.5. The most prominent peaks are 3066 cm^{-1} (aromatic C-H stretch), 2857 cm^{-1} (aliphatic C-H stretch), 1698 and 1679 cm^{-1} (Imide C=O Stretch), 1581 cm^{-1} (C=C stretch), 1345 cm^{-1} (C-N stretch), 1260 cm^{-1} (C-O Stretch), 1095 cm^{-1} (P-O-C Stretch) and 766 cm^{-1} for (P-O).

If we compare between anhydride peak at 1765 cm^{-1} , we can see that the described peak was being replaced by the imide peaks at 1698 and 1679 cm^{-1} . More vitally, peak at the 1345 cm^{-1} for C-N confirms the formation of the imide.

5.2 Synthesis of N,N'-bis(7H-purinyl)-1,4,5,8-naphthalene diimide (5) and IR Spectra Analysis

N,N'-bis(7H-purinyl)-1,4,5,8-naphthalene diimide (5) was synthesized successfully according to the Figure of 3.2. Purifying techniques such as chloroform soxhlet was used in order to get rid of the amine and recrystallization technique by using DMSO and water to get rid of high boiling solvent. The color of the compound is greenish brown with the yield of 65.2 %.

Analysis of FT-IR can be seen in Figure 4.4, the main characteristic peaks are 3064 cm^{-1} (aromatic C-H Stretch), 1703 and 1683 cm^{-1} (Imide C=O stretch), 1591 cm^{-1} (aromatic C=C stretch), 1333 cm^{-1} (C-N stretch) and 756 cm^{-1} for C-H aromatic bending.

As we make a comparison between the spectrum of 1 and 5, we are able to see that the peak for anhydride at 1765 is disappeared and replaced by C=O imide peaks at 1703 and 1683 cm^{-1} and formation of the peak of C-N at 1333 cm^{-1} , which is a marvelous clue for the formation of imide.

5.3 Solubility of the 3 and 5

Solubility of 3 and 5 can be seen in detail in the below table. Generally, both of them are fairly soluble in polar aprotic solvents such as DMF, DMSO, DMAc and NMP. Also, they are soluble in TFAc. Moreover, they are insoluble in polar aprotic solvent such as acetonitrile.

Table 5.1: Solubility test of 1, 3 and 5

Solubility/ color			
Solvents	1	3	5
CHL	-- / Colorless	-- / Colorless	-- / Colorless
TFAc	++ / Pale yellow	++ / Dark color	++ / Brown color
NMP	+ - / Pale green	- + / Light yellow	++ / Light brown
DMF	+ - / Pale pink	- + / Light yellow	+ - / Light brown
DMAc	+ - / Pale green	- + / Light yellow	+ - / Light brown
DMSO	-- / Colorless	- + / Brown yellow	+ - / Light brown
Water	-- / Colorless	-- / Colorless	- + / Light brown

Measured at concentration of 10 mg mL⁻¹ in solvents at 25°C. (+ +): Soluble at room temperature, (– –) Insoluble, (+ –) mostly soluble at high temperature 70°C (5-10 mg mL⁻¹), (– +) Soluble after putting in sonicator at high temperature. TFAc; Trifloro acetic acid; NMP: N-methyl pyrrolidine; DMF: N,N-dimethylformamide; DMSO: dimethyl sulfoxide; DMAc: dimethylacetamide

5.4 Interpretation of UV / Vis absorption for 3 and 5

The optical property of 3 and 5 is calculated by UV / Vis absorption in various solvents ranging from nonpolar to polar protic and aprotic to see different interactions between them. Data which has been achieved is used to find out vital photophysical parameters and they are being put in Table 4.9.

About compound 3, from figure 4.10 till 4.14 two absorption peaks can be seen for all of them which belong to $\pi-\pi^*$ transitions of NDI from $0 \rightarrow 1$ and $0 \rightarrow 0$. Except in

TFAc, a small peak, a shoulder, after 400 nm can be seen for all of them which most probably due to aggregation.

Generally, only one prominent peak was observed for 5 in different solvents which most probably because of electron transfer between imide (acceptor) and amine group (donor) , (Charge transfer complex), and intermolecular interaction. In higher polar aprotic solvents such as (DMSO and DMF), the peak goes toward red shift (bathochromic shift) with the values 362 nm and 368 nm in turn. More interestingly, since TFAc is considered to be polar protic solvent so it can form H-bond with the compound and the peak goes toward hypsochromic shift since more energy is required to excite the electrons and it can be seen at 362 nm. In CHL, few shoulders can be seen which most probably due to aggregation of the solution.

Chapter 6

CONCLUSION

In the present work, two novel diimides, N,N'-bis[(2-(dihydrogenphosphoryl)ethyl)]-1,4,5,8-naphthalene diimide (3) and N,N'-bis(7H-purinyl)-1,4,5,8-naphthalene diimide (5) have been successfully synthesized by condensation in high yield.

The qualitative solubility properties are investigated in various organic solvents. Accordingly, compounds 3 and 5 are both soluble in the polar aprotic solvents such as DMF, DMSO and DMAc. In addition, they do not dissolve in nonpolar solvents such as chloroform.

The optical properties of the compounds have been studied widely by using UV/Vis absorption spectroscopic method. Interestingly, different absorption characteristics were observed in various solvents owing to different intermolecular interactions. Compound 3 has shown 2 peaks in UV/Vis, whereas compound 5 has displayed 1 peak in it. Usually, NDI shows 3 peaks but in my case we are expecting that charge transfer complex causes this phenomena. Compound 5 has displayed high molar absorptivity in polar aprotic solvents especially in DMAc due to strong intra and intermolecular interactions between solute-solvent in polar solvents. Moreover, from FT-IR, the anhydride peak for NDA at 1765 cm^{-1} is being replaced by C=O imide stretching at 1698 cm^{-1} and 1679 cm^{-1} for 3 and 1703 cm^{-1} and 1683 cm^{-1} for 5 and formation of

C–N at 1345 cm^{-1} for 3 and at 1333 cm^{-1} for 5 is a good clue to decide that the imide has been produced.

The yield for 5 is not as high as 3 because further purification process was done for 5 than 3. For instance, recrystallization by DMSO was done three times for 5 but only 1 time for 3 and usually while purification some quantity of compound can be lost.

As a future work, compounds 3 and 5 will be applied in medical aspects as a probable anticancer owing to the planarity, rigidity, easy synthesis and good solubility. Especially, both 3 and 5 can have excellent ability to interact through intermolecular hydrogen bonding and π – π interactions with the guanine quadruplex and inhibit the function of telomerase and then stop proliferating of malignant cells. Moreover, it can also be applied in photonic applications.

REFERENCES

- Alberts, B., Johnson, A., Lewis, J., Raff, M., Roberts, K., & Walter, P. (2002). The shape and structure of proteins. *In Molecular Biology of the Cell. 4th edition. Garland Science.*
- Al Kobaisi, M., Bhosale, S. V., Latham, K., & Raynor, A. M. (2016). Functional naphthalene diimides: synthesis, properties, and applications. *Chemical Reviews*, 116(19), 11685-11796. <https://doi.org/10.1021/acs.chemrev.6b00160>
- Aleshinloye, A. O., Bodapati, J. B., & Icil, H. (2015). Synthesis, characterization, optical and electrochemical properties of a new chiral multichromophoric system based on perylene and naphthalene diimides. *Journal of Photochemistry and Photobiology a-Chemistry*, 300, 27-37. <https://doi.org/10.1016/j.jphotochem.2014.12.007>
- Ang, D. L., Harper, B. W. J., Cubo, L., Mendoza, O., Vilar, R., & Aldrich-Wright, J. (2016). Quadruplex DNA-stabilising dinuclear platinum(II) terpyridine complexes with flexible linkers. *Chemistry-a European Journal*, 22(7), 2317-2325. <https://doi.org/10.1002/chem.201503663>
- Asamitsu, S., Bando, T., & Sugiyama, H. (2019). Ligand design to acquire specificity to intended g-quadruplex structures. *Chemistry-a European Journal*, 25(2), 417-430. <https://doi.org/10.1002/chem.201802691>

- Asamitsu, S., Obata, S., Yu, Z. T., Bando, T., & Sugiyama, H. (2019). Recent progress of targeted g-quadruplex-preferred ligands toward cancer therapy. *Molecules*, 24(3), Article 429. <https://doi.org/10.3390/molecules24030429>
- Bhosale, S. V., & Bhargava, S. K. (2012). Recent progress of core-substituted naphthalenediimides: highlights from 2010. *Organic & Biomolecular Chemistry*, 10(32), 6455-6468. <https://doi.org/10.1039/c2ob25798j>
- Bhosale, S. V., Jani, C. H., & Langford, S. J. (2008). Chemistry of naphthalene diimides. *Chemical Society Reviews*, 37(2), 331-342. <https://doi.org/10.1039/b615857a>
- Burton, J. D. (2005). The mtt assay to evaluate chemosensitivity. *In Chemosensitivity (pp. 69-78). Humana Press*. <https://doi.org/10.1385/1-59259-869-2:069>
- Bray, F., Ferlay, J., Soerjomataram, I., Siegel, R. L., Torre, L. A., & Jemal, A. (2018). Global cancer statistics 2018: GLOBOCAN estimates of incidence and mortality worldwide for 36 cancers in 185 countries. *Ca-a Cancer Journal for Clinicians*, 68(6), 394-424. <https://doi.org/10.3322/caac.21492>
- Cao, Y., DePinho, R. A., Ernst, M., & Vousden, K. (2011). Cancer research: past, present and future. *Nature Reviews Cancer*, 11(10), 749-754. <https://doi.org/10.1038/nrc3138>

- Doll, R., & Peto, R. (1981). The causes of cancer - quantitative estimates of avoidable risks of cancer in the united states today. *Jnci-Journal of the National Cancer Institute*, 66(6), 1191-+. <https://doi.org/10.1093/jnci/66.6.1192>
- Doria, F., Nadai, M., Costa, G., Sattin, G., Gallati, C., Bergamaschi, G., . . . Richter, S. N. (2016). Extended naphthalene diimides with donor/acceptor hydrogen-bonding properties targeting g-quadruplex nucleic acids. *European Journal of Organic Chemistry*, 2016(28), 4824-4833. <https://doi.org/10.1002/ejoc.201600757>
- Doria, F., Nadai, M., Folini, M., Di Antonio, M., Germani, L., Percivalle, C., . . . Freccero, M. (2012). Hybrid ligand-alkylating agents targeting telomeric g-quadruplex structures. *Organic & Biomolecular Chemistry*, 10(14), 2798-2806. <https://doi.org/10.1039/c2ob06816h>
- Doria, F., Salvati, E., Pompili, L., Pirota, V., D'Angelo, C., Manoli, F., . . . Freccero, M. (2019). Dyads of g-quadruplex ligands triggering DNA damage response and tumour cell growth inhibition at subnanomolar concentration. *Chemistry-a European Journal*, 25(47), 11085-11097. <https://doi.org/10.1002/chem.201900766>
- Esaki, Y., Islam, M. M., Fujii, S., Sato, S., & Takenaka, S. (2014). Design of tetraplex specific ligands: cyclic naphthalene diimide. *Chemical Communications*, 50(45), 5967-5969. <https://doi.org/10.1039/c4cc01005a>

- Gao, L., Ge, C. C., Wang, S. Z., Xu, X. J., Feng, Y. L., Li, X. N., . . . Xie, S. Q. (2020). The role of p53-mediated signaling in the therapeutic response of colorectal cancer to 9F, a spermine-modified naphthalene diimide derivative. *Cancers*, *12*(3), Article 528. <https://doi.org/10.3390/cancers12030528>
- Ghule, N. V., Bhosale, R. S., Kharat, K., Puyad, A. L., & Bhosale, S. V. (2015). A naphthalenediimide-based luorescent sensor for detecting the ph within the rough endoplasmic reticulum of living cells. *Chempluschem*, *80*(3), 485-489. <https://doi.org/10.1002/cplu.201402307>
- Guha, S., Goodson, F. S., Corson, L. J., & Saha, S. (2012). Boundaries of anion/naphthalenediimide interactions: from anion-pi interactions to anion-induced charge-transfer and electron-transfer phenomena. *Journal of the American Chemical Society*, *134*(33), 13679-13691. <https://doi.org/10.1021/ja303173n>
- Guha, S., & Saha, S. (2010). Fluoride ion sensing by an anion-pi interaction. *Journal of the American Chemical Society*, *132*(50), 17674-17677. <https://doi.org/10.1021/ja107382x>
- Gunaratnam, M., Collie, G. W., Reszka, A. P., Todd, A. K., Parkinson, G. N., & Neidle, S. (2018). A naphthalene diimide g-quadruplex ligand inhibits cell growth and down-regulates BCL-2 expression in an imatinib-resistant gastrointestinal cancer cell line. *Bioorganic & Medicinal Chemistry*, *26*(11), 2958-2964. <https://doi.org/10.1016/j.bmc.2018.04.050>

- Hampel, S. M., Pepe, A., Greulich-Bode, K. M., Malhotra, S. V., Reszka, A. P., Veith, S., . . . Neidle, S. (2013). Mechanism of the antiproliferative activity of some naphthalene diimide g-quadruplex ligands. *Molecular Pharmacology*, 83(2), 470-480. <https://doi.org/10.1124/mol.112.081075>
- Hanahan, D., & Weinberg, R. A. (2011). Hallmarks of cancer: the next generation. *Cell*, 144(5), 646-674. <https://doi.org/10.1016/j.cell.2011.02.013>
- Hausman, D. M. (2019). What is cancer? *Perspectives in Biology and Medicine*, 62(4), 778-784.
- Hornberg, J. J., Bruggeman, F. J., Westerhoff, H. V., & Lankelma, J. (2006). Cancer: a systems biology disease. *Biosystems*, 83(2-3), 81-90. <https://doi.org/10.1016/j.biosystems.2005.05.014>
- Huppert, J. L. (2008). Four-stranded nucleic acids: structure, function and targeting of g-quadruplexes. *Chemical Society Reviews*, 37(7), 1375-1384. <https://doi.org/10.1039/b702491f>
- Hurley, L. H. (2002). DNA and its associated processes as targets for cancer therapy. *Nature Reviews Cancer*, 2(3), 188-200. <https://doi.org/10.1038/nrc749>
- Ke, H., Wang, L., Chen, Y., Lin, M. J., & Chen, J. Z. (2014). Electron-deficient naphthalene diimides as efficient planar pi-acid organocatalysts for selective oxidative C-C coupling of 2,6-di-tert-butylphenol: a temperature effect.

Journal of Molecular Catalysis a-Chemical, 385, 26-30.
<https://doi.org/10.1016/j.molcata.2014.01.014>

Mancini, J., Rousseau, P., Castor, K. J., Sleiman, H. F., & Autexier, C. (2016). Platinum(II) phenanthroimidazole g-quadruplex ligand induces selective telomere shortening in A549 cancer cells. *Biochimie*, 121, 287-297.
<https://doi.org/10.1016/j.biochi.2015.12.015>

Mareda, J., & Matile, S. (2009). Anion- π slides for transmembrane transport [Article]. *Chemistry-a European Journal*, 15(1), 28-37.
<https://doi.org/10.1002/chem.200801643>

Martinez, R., & Chacon-Garcia, L. (2005). The search of DNA-intercalators as antitumoral drugs: what it worked and what did not work. *Current Medicinal Chemistry*, 12(2), 127-151. <https://doi.org/10.2174/0929867053363414>

McCauley, J., Zivanovic, A., & Skropeta, D. (2013). Bioassays for anticancer ctivities. *Metabolomics Tools for Natural Product Discovery: Methods and Protocols*, 1055, 191-205. https://doi.org/10.1007/978-1-62703-577-4_14

Micco, M., Collie, G., Gunaratnam, M., Ohnmacht, S. A., Reszka, A. P., & Neidle, S. (2012). Structure-based design of g-quadruplex ligands leads to enhanced potency against pancreatic cancer cells. *Cancer Research*, 72. <https://doi.org/10.1158/1538-7445.am2012-lb-2>

- Murat, P., Singh, Y., & Defrancq, E. (2011). Methods for investigating g-quadruplex DNA/ligand interactions. *Chemical Society Reviews*, 40(11), 5293-5307. <https://doi.org/10.1039/c1cs15117g>
- Nadai, M., Doria, F., Di Antonio, M., Sattin, G., Germani, L., Percivalle, C., . . . Freccero, M. (2011). Naphthalene diimide scaffolds with dual reversible and covalent interaction properties towards g-quadruplex. *Biochimie*, 93(8), 1328-1340. <https://doi.org/10.1016/j.biochi.2011.06.015>
- Nadai, M., Doria, F., Scalabrin, M., Pirota, V., Grande, V., Bergamaschi, G., . . . Freccero, M. (2018). A catalytic and selective scissoring molecular tool for quadruplex nucleic acids. *Journal of the American Chemical Society*, 140(44), 14528-14532. <https://doi.org/10.1021/jacs.8b05337>
- Ozser, M. E., Uzun, D., Elci, I., Icil, H., & Demuth, M. (2003). Novel naphthalene diimides and a cyclophane thereof: synthesis, characterization, photophysical and electrochemical properties. *Photochemical & Photobiological Sciences*, 2(3), 218-223. <https://doi.org/10.1039/b208856h>
- Polander, L. E., Romanov, A. S., Barlow, S., Hwang, D. K., Kippelen, B., Timofeeva, T. V., & Marder, S. R. (2012). Stannyl derivatives of naphthalene diimides and their use in oligomer synthesis. *Organic Letters*, 14(3), 918-921. <https://doi.org/10.1021/ol203432x>
- Prato, G., Silvent, S., Saka, S., Lamberto, M., & Kosenkov, D. (2015). Thermodynamics of binding of di- and tetrasubstituted naphthalene diimide

ligands to DNA g-quadruplex. *Journal of Physical Chemistry B*, 119(8), 3335-3347. <https://doi.org/10.1021/jp509637y>

Sato, N., Takahashi, S., Tateishi-Karimata, H., Hazemi, M. E., Chikuni, T., Onizuka, K., . . . Nagatsugi, F. (2018). Alkylating probes for the g-quadruplex structure and evaluation of the properties of the alkylated g-quadruplex DNA. *Organic & Biomolecular Chemistry*, 16(9), 1436-1441. <https://doi.org/10.1039/c7ob03179c>

Sato, S., Kondo, H., Nojima, T., & Takenaka, S. (2005). Electrochemical telomerase assay with ferrocenyl naphthalene diimide as a tetraplex DNA-specific binder. *Analytical Chemistry*, 77(22), 7304-7309. <https://doi.org/10.1021/ac0510235>

Seeman, N. C. (2003). DNA in a material world. *Nature*, 421(6921), 427-431. <https://doi.org/10.1038/nature01406>

Senthilraja, P., & Kathiresan, K. (2015). In vitro cytotoxicity mtt assay in vero, HepG2 and MCF-7 cell lines study of marine yeast. *J Appl Pharm Sci*, 5(3), 80-4. <http://dx.doi.org/10.7324/JAPS.2015.50313>

Sommer, M. (2014). Conjugated polymers based on naphthalene diimide for organic electronics. *Journal of Materials Chemistry C*, 2(17), 3088-3098. <https://doi.org/10.1039/c3tc31755b>

Sun, D. Y., Thompson, B., Cathers, B. E., Salazar, M., Kerwin, S. M., Trent, J. O., . . . Hurley, L. H. (1997). Inhibition of human telomerase by a g-quadruplex-

interactive compound. *Journal of Medicinal Chemistry*, 40(14), 2113-2116.
<https://doi.org/10.1021/jm970199z>

Sun, M. M., Mullen, K., & Yin, M. Z. (2016). Water-soluble perylenediimides: design concepts and biological applications. *Chemical Society Reviews*, 45(6), 1513-1528. <https://doi.org/10.1039/c5cs00754b>

Takeuchi, R., Zou, T. T., Wakahara, D., Nakano, Y., Sato, S., & Takenaka, S. (2019). Cyclic naphthalene diimide dimer with a strengthened ability to stabilize dimeric G-quadruplex. *Chemistry-a European Journal*, 25(37), 8691-8695.
<https://doi.org/10.1002/chem.201901468>

Tandon, R., Luxami, V., Kaur, H., Tandon, N., & Paul, K. (2017). 1,8-naphthalimide: a potent DNA intercalator and target for cancer therapy. *Chemical Record*, 17(10), 956-993. <https://doi.org/10.1002/tcr.201600134>

Tassinari, M., Cimino-Reale, G., Nadai, M., Doria, F., Butovskaya, E., Recagni, M., . . . Folini, M. (2018). Down-regulation of the androgen receptor by G-quadruplex ligands sensitizes castration-resistant prostate cancer cells to enzalutamide. *Journal of Medicinal Chemistry*, 61(19), 8625-8638.
<https://doi.org/10.1021/acs.jmedchem.8b00502>

Tumiatti, V., Milelli, A., Minarini, A., Micco, M., Campani, A. G., Roncuzzi, L., . . . Melchiorre, C. (2009). Design, synthesis, and biological evaluation of substituted naphthalene imides and diimides as anticancer agent. *Journal of Medicinal Chemistry*, 52(23), 7873-7877. <https://doi.org/10.1021/jm901131m>

Tumiatti, V., Milelli, A., Minarini, A., Rosini, M., Bolognesi, M. L., Micco, M., . . .

Melchiorre, C. (2008). Structure-activity relationships of acetylcholinesterase noncovalent inhibitors based on a polyamine backbone. 4. further investigation on the inner spacer. *Journal of Medicinal Chemistry*, 51(22), 7308-7312.
<https://doi.org/10.1021/jm8009684>

Van Raamsdonk, C. D., Bezrookove, V., Green, G., Bauer, J., Gaugler, L., O'Brien, J.

M., . . . Bastian, B. C. (2009). Frequent somatic mutations of gnaq in uveal melanoma and blue naevi. *Nature*, 457(7229), 599-U108.
<https://doi.org/10.1038/nature07586>

Vasimalla, S., Sato, S., Takenaka, F., Kurose, Y., & Takenaka, S. (2017). Cyclic

perylene diimide: selective ligand for tetraplex DNA binding over double stranded DNA. *Bioorganic & Medicinal Chemistry*, 25(24), 6404-6411.
<https://doi.org/10.1016/j.bmc.2017.10.014>

Weinberg, R. A. (1996). How cancer arises. *Scientific American*, 275(3), 62-70.

<https://doi.org/10.1038/scientificamerican0996-62>

Whitesides, G. M., Simanek, E. E., Mathias, J. P., Seto, C. T., Chin, D. N., Mammen,

M., & Gordon, D. M. (1995). Noncovalent synthesis - using physical-organic chemistry to make aggregates. *Accounts of Chemical Research*, 28(1), 37-44.
<https://doi.org/10.1021/ar00049a006>

Yue, W., Zhen, Y. G., Li, Y., Jiang, W., Lv, A. F., & Wang, Z. H. (2010). One-pot synthesis of well-defined oligo- butadiynylene-naphthalene diimides. *Organic Letters*, 12(15), 3460-3463. <https://doi.org/10.1021/ol101280e>

Zahler, A. M., Williamson, J. R., Cech, T. R., & Prescott, D. M. (1991). Inhibition of telomerase by g-quarteplex DNA structures. *Nature*, 350(6320), 718-720. <https://doi.org/10.1038/350718a0>

Zhan, X. W., Facchetti, A., Barlow, S., Marks, T. J., Ratner, M. A., Wasielewski, M. R., & Marder, S. R. (2011). Rylene and related diimides for organic electronics. *advanced materials*, 23(2), 268-284. <https://doi.org/10.1002/adma.201001402>